Ice Island Study

Final Report

MMS Project #468

Prepared for:

Minerals Management Service
US Department of the Interior

Prepared by:

C-CORE

C-CORE Report:

R-05-014-241v1.0
August 2005

C-CORE
Captain Robert A Bartlett Building
Morrissey Road
St. John's, NL
Canada A1B 3X5

T: (709) 737-8354
F: (709) 737-4706

info@c-core.ca
www.c-core.ca

The correct citation for this report is:

C-CORE (2005). Ice Island Study. Final Report. Prepared for Minerals Management Service, US Department of the Interior. Prepared by C-CORE. Report No. R-05-014-241 v1.0, August 2005

Project Team:

Vincent Morgan (C-CORE, Project Manager)
Jack Clark (C-CORE)
Jim Bruce (C-CORE)
Elaine Martin (C-CORE)
Dan Masterson (Sandwell Engineering)
Ken Croasdale (K.R. Croasdale & Associates)

EXECUTIVE SUMMARY

This report summarises the issues related to the use of man-made ice islands as exploration drilling structures in the Canadian Arctic Islands and Beaufort Sea. The historical development of ice island technology has been reviewed with respect to design, construction and maintenance issues relating to the use of both floating and grounded islands. The report includes the opinion of a number of experts who, between them, have had direct involvement in all ice islands constructed in North America. This experience has been utilized in the form of contribution to, and review of the report.

A review of the use of experimental and operational ice islands, primarily in the Beaufort Sea, clearly demonstrates the advantages of spray ice production over other methods of construction, such as gravel islands or flooded ice production. Achievable cost savings are significant as a result of using a natural material with no transportation costs, and high build up rates allow construction times to be minimized.

One critical design consideration for grounded ice islands is the determination of the ice loads applied to the island by the surrounding ice sheet. There is a significant difference in determining the ice crushing loads between the various codes of practice available to the industry, which can result in significant variations in final design parameters. A number of potential failure mechanisms have been investigated, which suggests that the limiting criteria may be either crushing of the ice sheet or edge failure at the interface between natural and spray ice, depending on site specific parameters.

Spray ice production technology has been developed over the past 30 years to meet the requirements of the industry, particularly prior to 1986 when exploration activity was high in the Beaufort Sea. The range of pump and nozzle configurations used in practice has been reviewed to establish the parameters required to produce spray ice in an efficient manner. Efficiency generally improves by using larger pumps, which allows individual particles to remain in flight for longer thereby undergoing greater heat transfer. Build up rates are also maximized by using large flow rate pumps. Constraints to operational efficiency due to wind and temperature variations have also been considered.

Potential improvements to ice island technology have been investigated, such as their use in deeper water and potential for extending the available drilling season. The use of off-ice construction techniques, along with marine demobilization has been shown to potentially achieve improvements with respect to both of these objectives. Issues relating to ablation and edge erosion of ice islands at the end of the winter season have been investigated, including a brief evaluation of the requirements to allow an island to remain in place on a multi-year basis. The changes in temperature regime as a result of climate change over the past 30 years have been reviewed. This suggests that although there is a large variability in conditions year-to-year, the trends do not suggest that the use of ice island construction in the Western Artic will be impeded by this over at least the next decade.

The use of innovative methods to further improve efficiencies in design and construction have been presented, some of which may warrant further development. Methods include the use of alternative ice production techniques when weather conditions are unsuitable for spray ice production, methods of reducing ice loads through suppressing natural ice thickness, and the use of structures to form rubble piles to reduce the required spray ice volume. All these techniques could have uses in appropriate conditions for improving efficiency and reducing risk and cost associated with spray ice construction.

The performance of a centrifuge model test has demonstrated the potential applicability of this technique to investigate ice island performance. The test simulated ice loading on an island to produce sliding failure, and compared the results with the calculated capacity. The test results showed that under the conditions tested, the island deformed by failure of the ice core rather than by sliding along the seabed as predicted. The measured loads were greater than calculated, suggesting that current design methods could be optimized to further reduce cost. The use of centrifuge technology could be used to improve understanding and further development of design issues.

A number of potential areas suitable for further research have been identified as a result of the review presented in this report. A list of issues has been identified on the basis that improvements in these areas could lead to significant efficiencies in terms of reduced risk or reduced cost. A consensus on the issues most likely to provide substantial improvements for the use of ice islands for offshore Arctic exploration could be developed through a forum with invited participants from industry, academia and government agencies. The main issues identified comprise the following:

- Ice sheet failure mechanics during impact with grounded structures.
- Sliding resistance of grounded ice islands.
- Ice island distortion during loading events.
- Feasibility of construction of ice islands in deeper water environments.
- Further study of the deterioration of ice island structures after the winter drilling season. Feasibility of ice island survival to allow multi-year operations.
- Construction management techniques to allow improved feedback of construction related issues to the design.
- Spray ice strength characteristics

TABLE OF CONTENTS

LIST OF TABLES

LIST OF FIGURES

1.0 TERMS & SYMBOLS

1.1 Glossary

A glossary of terms used in this report is presented in this section. The included terminology has been identified on the basis of technical engineering terms and phrases used in this report related to the use of man-made ice islands for oil and gas exploration.

Ablation	The melting process by which ice thickness is reduced through radiation, conduction and convection effects.
Beaufort Gyre	The rotating current in the Arctic Ocean that causes the Polar Pack to rotate slowly in a clockwise direction.
Build-up Rate	The production rate at which artificial ice is formed – defined either as vertical increase in height or volume production.
CIDS	Concrete Island Drilling Structure – mobile bottom-founded drilling structure used in the US Beaufort Sea in harsh ice environments.
CRI	Caisson Retained Island – bottom-founded island constructed within a caisson structure for exploration drilling in the Beaufort Sea in harsh ice environments.
Columnar Ice	Ice that has been formed with preferential crystal orientation, usually in the vertical direction as a result of a 1-dimensional freezing process. This results in non-isotropic ice properties in the direction of the crystal elongation.
Creep Settlement	Settlement of the ice surface or structures supported on ice due to creep under sustained loading conditions.
Crushing Failure	Failure of the ice sheet due to crushing of the ice as compressive load is applied.
Edge Erosion	The removal of ice from the edge of an ice island due to mechanical and thermal action of the surrounding seawater.
Fall Freeze-up	The start of significant ice accumulation at the start of the winter season as a result of falling air temperatures. Ice formation starts as temperatures drop consistently below freezing in September, with significant nearshore ice build-up occurring from October.
First Year Ice	Ice that has formed during the current winter season, it has a

	relatively high salinity and low strength compared to older ice.
Floating Ice Island	Artificial ice island that is not in contact with the seafloor, but floats and is held in place within stable landfast ice.
Flooded Ice	Ice that has been formed artificially by placing water and allowing it to freeze as a result of the cold ambient temperatures.
Freeboard	Height of a platform or deck of a grounded or floating structure or vessel above sea level.
Granular Ice	Ice which has been formed with randomly oriented crystals, resulting in isotropic properties.
Grounded Ice Island	Artificial ice island that is in contact with the seafloor and derives stability through sliding resistance with the seabed soil material.
Glacial Ice	Ice that is formed from compressed snow and eventually becomes separated from the edge of the glaciers to form icebergs or natural ice islands.
Ice Floe	A large piece of ice that has separated from the main ice pack.
Ice Island	Mass of ice formed artificially for use to support a rig and associated equipment for drilling operations.
Ice Protection Structure	Mass of ice formed artificially to provide protection to drilling structures and reduce the loads from the surrounding ice sheet.
Ice Road	Transportation route constructed on stable landfast ice to allow access to offshore locations. The road may be floating or grounded, and be constructed using flooding or spraying techniques.
Ice Rafting	A process in which a section of ice sheet rides over an adjacent section, resulting in increased thickeness. This is usually caused by wind effects acting on relatively thin first year ice.
Ice Ridging	A process in which initially level ice is crushed due to impact or other events to form a zone, usually a linear feature, of thickened ice comprising a sail above water and a keel under water.
Ice Rubble	The accumulation of ice mass as a result of continuous action of mobile ice building up on previously grounded ice features.
Insitu Testing	Techniques used to establish ice or soil properties in place

	without removing samples. This ensures that the material being tested remains in its original condition during testing without disturbance.
Kigoriak	Ice breaking vessel used as part of experimental ice island and protection barrier experiments in the Beaufort Sea.
Laboratory Testing	Testing technique in which samples of ice or soil are recovered and taken to a laboratory for testing. Sampling causes disturbance of the material, but laboratory testing conditions can provide important additional information about the material.
Landfast Ice	Ice that is frozen in place by contact with the coastline and also held in place by grounded features in the shallow water environment.
Multi Year Ice	Ice that has survived at least one summer season, it usually has lower salinity and higher strength than first year ice.
Off-Ice Construction	The process of ice island construction using fixed or floating platforms or vessels to house the ice forming equipment, which does not require stable ice conditions for support.
On-Ice Construction	The process of ice island construction using ice forming equipment supported directly on the stable landfast ice.
Passive Edge Failure	Potential failure mechanism in which the edge of an ice island fails as a result of ice sheet interaction, causing a wedge of ice to detach and move up or down relative to the main island body.
Polar Ice Pack	Permanent multi year ice body situated in the Arctic Basin.
Relief Well Pad	Secondary drilling location constructed for use as a drilling platform in the case of a blow out of the primary well. Legislation requires that same season relief well capability is provided for the first exploration well into a particular play.
SSDC	Single Steel Drilling Caisson– mobile bottom-founded drilling structure used in the US and Canadian Beaufort Sea in harsh ice environments.
Shear failure	Potential internal failure mechanism within an ice island due to shear failure of the ice as a result of load applied by the surrounding ice sheet.
Shear Zone	A section of ice at the edge of the landfast ice, which is active and

	mobile, resulting in potentially large movements as a result of winds and currents. The ice is a mix of first year and multi year ice.
Sliding Resistance	The resistance provided by the ice/seabed interaction to prevent lateral movement of an ice island as load is applied by the surrounding ice sheet.
Spray Ice	Ice that has been formed artificially by spraying water into the air and allowing to freeze prior to reaching the surface as a result of the cold ambient temperatures.
Spray Monitor	Nozzle used to direct high pressure water jets into the air for the production of spray ice.
Spray Pump	Pump used to spray water into the air for the production of spray ice. Typical pumps currently used for this purpose are rated at 100 to 330 l/s flowrate and 1200kPa operating pressure.
Spray Ice Efficiency	Ratio of water pumped (or sprayed) to ice formed as part of the production process. May be defined in terms of volume or weight, taking into account the difference in density between water and ice. May also account for lower efficiency due to ice that forms but does not remain within the target area.
Spring Break-up	The start of significant ice deterioration due to warming air temperature. Ice melting starts with the onset of consistent above freezing temperatures in May, with significant open water starting in early July.
Thermal Events	The expansion or contraction of ice due to changes in temperature, which can cause significant stress and load buildup on fixed structures located within the ice .
Well Cellar	The location under the drill rig at which the drill string penetrates the drill deck or platform.

1.2 Symbols

A list of symbols used within the report is presented in this section. Most symbols used in the equations presented in the report are valid for both SI and USCS units.

A	Constant derived from creep test
β_d	Below water slope of island edge
β_u	Above water slope of island edge
b	Loading radius of a structure
B	Constant exponent of stress derived from creep tests
c	Cohesion intercept of spray ice
c_u	Undrained shear strength of seabed soil
C	Constant exponent of time derived from creep tests
Cp	Empirical constant for ice load calculation
δ	Foundation deflection (settlement)
d	Water depth
D_c	Ice island core diameter
Dp	Empirical constant for ice load calculation
ε_e	Strain
E	Elastic modulus of the ice sheet
E^*	Longterm elastic modulus of ice to account for creep
Ep	Empirical constant for ice load calculation
F_c	Crushing failure of level ice per unit width
F_e	Failure load due to passive edge failure
g	Gravitational constant ($9.81 m/s^2$)
η	Porosity of spray ice
h_i	Ice sheet thickness
H	Height of the island above sea level (freeboard)
k	Unit weight of water
l	Stiffness length for calculation of floating island deflection
ϕ	Angle of internal friction of ice
ϕ_s	Angle of internal friction of soil
p_{eff}	Effective ice pressure
P	Applied load from a supported structure
ρ_w	Sea water density
ρ_i	Above water density of spray ice
ρ_{si}	Below water density of spray ice
R_s	Sliding resistance of ice island
σ	Normal stress, or fibre stress under bending
τ	Shear stress developed along the failure plane
T	Time
υ	Poisson's ratio
W	Nominal contact width

1.3 Unit Conversions

SI units have been used by default throughout the report, although the equivalent USCS units have also been given where appropriate. Conversion factors for units used in this report are provided below:

1 litre (l)	=	0.264	gallon (US liquid)
1 litre/second (l/s)	=	0.264	gallon/second (gal/s)
1 litre/second (l/s)	=	15.84	gallon/minute (gal/min)
1 kilogram (kg)	=	2.205	pound (lb)
1 kilogram (kg)	=	0.0011	ton (2000lb)
1 kilonewton (kN)	=	224.8	pound (lb)
1 kilonewton (kN)	=	0.112	ton (2000lb)
1 kilonewton/metre (kN/m)	=	5.710	pound/inch (lbf/in)
1 kilopascal (kN/m^2 or kPa)	=	0.145	pound/sq inch (lbf/in^2)
1 kilonewton per $metre^3$ (kN/m^3)	=	0.0036	pound/cubic inch (lbf/in^3)
1 meganewton (MN)	=	112.4	ton (2000lb)
1 meganewton/metre (MN/m)	=	5710	pound/inch (lbf/in)
1 metre (m)	=	1.094	yard (yd)
1 metre (m)	=	3.281	foot (ft)
1 metre/second (m/s)	=	1.944	knot
1 metre/second (m/s)	=	3.281	foot/second (ft/s)
1 $metre/second^2$ (m/s^2)	=	3.281	$foot/second^2$ (ft/s^2)
1 $metre^2$ (m^2)	=	1.196	$yard^2$ (yd^2)
1 $metre^2$ (m^2)	=	10.76	$foot^2$ (ft^2)
1 $metre^3$ (m^3)	=	1.308	$yard^3$ (yd^3)
1 $metre^3$ (m^3)	=	35.32	$foot^3$ (ft^3)
1 $metre^3$ (m^3)	=	264.2	gallon (US liquid)

2.0 BACKGROUND

The modern era of engineering activity in the arctic has provided tests of endurance and initiative in overcoming the harsh and unique environment. In North America, scientific research and engineering knowledge started in earnest during the second world war when the arctic was considered of key strategic importance. The construction of roads, airstrips and fuel supply pipelines were all required to support these activities and were initially developed empirically based on experience developed from previous projects.

Ice has been identified as an important material for use in engineering structures. Its availability on a seasonal basis, and lack of long-term detrimental effects on the delicate landscape made it economical to use, as has been demonstrated through centuries of traditional activity by northern inhabitants.

The use of ice as a support material for offshore oil and gas exploration began in 1973 at the Hecla exploration well in the Canadian High Arctic. The floating drilling pad used artificial thickening of the natural ice sheet by flooding with seawater. Build-up rates where dictated by the time required to freeze thin layers of water, which were repeatedly added to the frozen core. Close to 40 floating ice pads were successfully used between 1973 and 1986 in the Canadian High Arctic using flooding and freezing techniques in water depths up to 500m (Masterson et al 1987).

Nearshore oil and gas exploration activities also started in the Beaufort Sea in the1970s. A wide range of structures has been used to allow offshore drilling, including floating drill ships, bottom founded structures, caisson-retained islands, gravel and sand non-retained islands and ice islands (Croasdale 1991). The first grounded flooded ice island was built by Union Oil in Harrison Bay, Alaska in 1976/77. Grounded ice islands have generally been constructed in less than 9m water depth. The use of sprinkling and spraying on experimental and relief well pads has allowed these methods to be developed with lower risk to project schedules. Spray ice was also used to form protection structures around grounded drilling structures such as the CIDS platform offshore Alaska in the mid 1980s.

Numerous experiments were performed by Exxon, Esso, Canmar and others to improve knowledge of spray ice construction techniques and physical properties. Full-scale test facilities were established and databases of performance criteria produced. The mechanics of spray ice behaviour were established and compared with previous work with other types of ice, although there is still a wide range of values used in current design practice.

3.0 OBJECTIVES

This objectives of this study were:

- To review the available data from research and operational activities with respect to ice island design, construction and maintenance;
- To define current state-of-practice based on most recent methodology and practical application;
- To identify Critical areas in which advances could be made through additional focused research.

The overall aim of the report is to contribute to the continued successful exploration of hydrocarbons in the Arctic offshore through increased efficiency and reduced cost.

4.0 SCOPE OF WORK

The project has been performed in three parts:

- Assimilation of all the available research, design, construction and maintenance history of ice islands and use of this data to identify current state-of-practice. The review has made use of data from public sources such as conference proceedings, regulatory applications, textbooks and university theses. This was useful in providing statistical information and a general level of detail. Information contained in non-public documents such as individual designs and proprietary (at the time of undertaking) research also allows the benefit to the project to be expanded to encompass practical details of the projects discussed.

- Identification of potential advances through focused research. The information obtained from the review of documented ice island activity has been used to identify gaps in the level of knowledge, or limitations in the current practical application for economical island construction and operation. The team of experts brought together for this project has developed this list for consideration for future research.

- Performance of a demonstration centrifuge model test. The geotechnical centrifuge is used for extensive experimental modeling of stress dependent processes in geotechnical and ice engineering. A demonstration test has been undertaken to investigate whether this technique can be beneficial to the development and use of ice islands. The test compared sliding resistance on a soft clay seabed between a flat solid base (gravity base structure) and a spray ice island. Current design methodology does not differentiate between the two and does not consider the effects of impregnation into the seabed to provide passive resistance.

Two reports were prepared as part of this project, based on experience of the team at Sandwell Engineering. These reports summarise the use of floating and grounded ice islands designed and constructed by Sandwell since the 1970s (Sandwell 2003a), and design and construction details of the Thetis ice islands in 2003 (Sandwell 2003b). These reports are included in Appendices A and B respectively.

This report discusses the results of the above study areas. Since the identification of potential future advances are closely based on previous experience of the industry, these are highlighted and discussed throughout the report, and summarized in Section 13 to form the basis for developing priorities for future research.

This report considers the technical solutions developed by the oil and gas industry in overcoming the challenges of exploration in the arctic offshore region. It is acknowledged that consideration of operational costs are important, and often an overriding concern, in determining the suitability of particular method of operation, however, detailed cost comparisons have not been undertaken as part of this project.

5.0 OPERATIONAL EXPERIENCE

5.1 General

Construction techniques using variations on flooded and spray ice techniques advanced significantly as part of the oil and gas exploration in the 1970s. It was recognized that the large risks associated with drilling schedules required that the island had to be ready to accept the rig at the earliest date possible to allow the maximum operating window. Winter drilling programs are controlled by the latest safe demobilization date for removing the rig from the ice prior to break-up, linked with the contingency to drill a relief well if required. Exploration wells may be required to have a same-season relief well capability in the case of a blowout. A relief pad must therefore be constructed and sufficient time allowed before the end of the season to drill the relief well. A typical operating season is given in Figure 5.1. Research has therefore been focused on reducing the construction time for the platform, as well as more fundamental work on ice properties that have a direct influence on design.

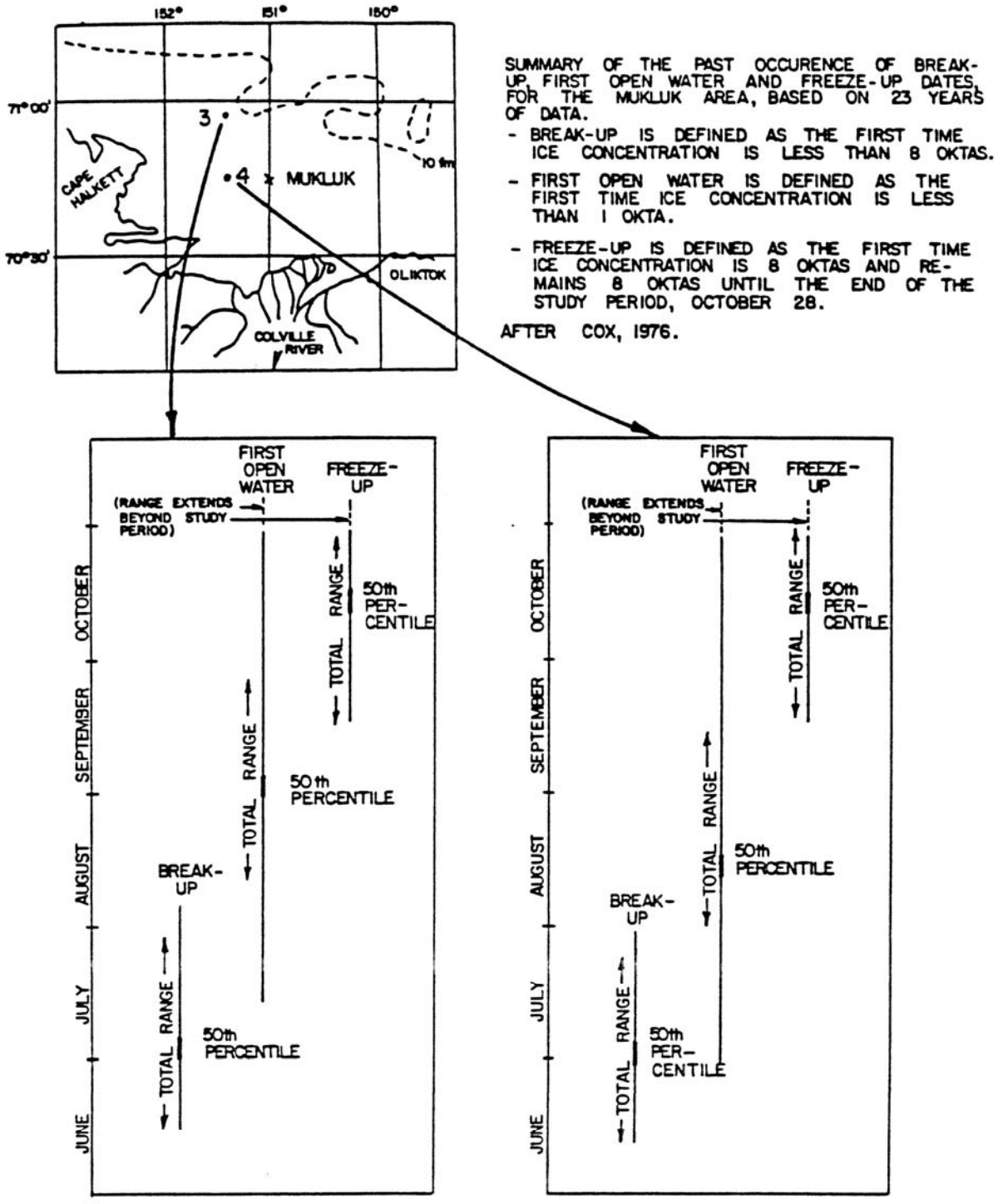

Figure 5.1: Typical Winter Season for Harrison Bay, Alaska (O'Rourke 1984)

5.2 Floating Ice Platforms

The floating Panarctic islands constructed between 1973 and 1986, were designed to limit the maximum extreme fibre stress beneath the rig to provide an adequate factor of safety against failure. They were also designed to provide sufficient freeboard so that rig settlement due to creep was controlled such that it remained above the waterline by an acceptable margin at the end of the drilling program.

Table 5.1 provides data on the floating drilling platforms constructed in the Canadian high Arctic over this time, and more detailed information is provided in Sandwell (20043a).

Table 5.1: Details of Floating ice Islands Constructed in Canadian High Arctic

Structure	Dates	Original Thickness	Design Thickness
Hecla N-52	1973/74	1.9 m	5.3 m
Resolute Bay Test	1974		
East Drake I-55	1974/5	2.0 m	5.0 m
NW Hecla M-25	1975/76	2.4 m	5.0 m
Jackson Bay G-16 & 16A	1975/76	1.2 m	5.5 m
W. Hecla P-62	1975/76	1.9 m	4.5 m
Drake F-76	1977/78	1.0 m	7.1 m
Roche Point O-43	1977/78	1.9 m	5.2 m
& Cape Grassy I-34	1977/78	0.9 m	5.3 m
Hazen Strait F-54	1978/79	2.1 m	6.5 m
Whitefish H-63	1978/79	6.3 m	6.4 m
Whitefish H-63A	1979/80	6.9 m	7.2 m
Char G-07	1980		
Baleana D-58	1980		
Cisco B-66	1980/81		~12 m
MacLean I-72	1980/81		5.6 m
Cisco C-42	1982/82		5.7 m
Cape Mamen F-24	1981	4.59 m	6.4 m
Sculpin K-08	1981/82	10.1 m	10.3 m
Seal Island Loating Road	1981/82	1.1 m	2.8 m
Whitefish A-26	1981/82	6.6 m	7.1 m
Cisco K-58	1982/83		
Grenadier A-26	1982/83	1.3 m	6.9 m
Skate C-59	1982/83		6.1 m
E Drake L-06	1982/83		6.2 m
N Buckingham N-69	1982/83		6.6 m
Cisco M-22	1983/84	5.5 m	7.0 m
Cape Alison	1984/85	0.9 m	6.9 m
N Cornwall N-49	1985/86	0.9 m	7.1 m

A total of 38 wells were drilled from floating ice pads between 1973 and 1986 (Masterson et al 1987). Equipment was transported by air to a nearby land-based staging area ahead of platform construction. Construction equipment and personnel camps were relocated to the on-ice location using helicopters towards late November when natural ice cover was sufficiently thick, stable and frozen in. Construction generally started in the last week of November or first week of December using flooding techniques. This process used pumps to place seawater onto the ice in thin layers, allowing them to freeze in place to increase the thickness of the ice sheet at the drilling location. The majority of the drilling pads were built on level first year ice of the order of 1 to 2m thick. A number of pads were built on thick multi-year ice, for which flooding was used to provide a smooth surface rather than to increase the thickness. Construction of the platform took between 20 to 75 days, with an average build-up rate of approximately 70mm/day. Build-up rates varied significantly as a function of temperature, wind speed and equipment used. The platform would generally be ready to accept the rig during January or February, allowing up to 100 days of drilling.

Although the main structure to be constructed was the drilling pad to support the rig and associated equipment, other important infrastructure included a relief pad for use in the event of blowout and an airstrip for both Twin Otter and Hercules aircraft.

Movement of the landfast ice sheet was not a great concern in the arctic islands, based on a number of years of historical data and the landlocked nature of the ice. The relatively large water depth provided some allowance for relative horizontal movement between the platform and seabed without distressing the riser. The requirement to respud the hole was noted at Jackson G-16/G-16A in 1974/75, although no details are provided on the implications of this occurrence on cost or schedule.

Since the freeboard of a floating ice island is related directly to the density difference between the ice and seawater, any reduction in ice density would provide a greater freeboard for a given volume or thickness. The use of polyurethane foam was trialed at Char G-07 and Maclean I-72 in 1980. At Maclean I-72, for example, the use of 550m^3 of low-density foam blocks embedded in the flooded ice allowed a reduction of 350mm ice thickness and reduced the weight of the platform by 500 tonnes. This had the effect of reducing the construction time and allowing the platform to carry an additional 500 tonnes of rig load for a given freeboard.

Spray ice started to be used for the construction of the floating Arctic island platforms in 1984/85 at Cape Alison and 1985/86 at North Cornwall. High pressure, high volume pumps and monitors were used to enhance the freezing rate of seawater to build up the ice platform thickness. The use of a chemical additive, AFA-6, was also trialed with a view of enhancing efficiency, although reports of its success are mixed. It is suggested that the concentration used at Cape Allison was too low to be effective (Masterson et al 1987), and greater concentrations may have been beneficial, particularly at warmer (>-30^{o}C) temperatures (Sandwell 2003a). The use of spray ice construction is claimed to have reduced the construction time by 14 days on that project. This is significant, both in

terms of direct construction cost and to provide an increased drilling window prior to spring break-up. Figure 5.2 presents a schematic of the Cape Alison floating ice island.

Offshore exploration drilling in the high arctic islands was discontinued in about 1986 due to a downturn in exploration spending by the oil and gas industry. Little additional research has since been carried out and made public that relates specifically to floating ice drilling platforms.

Figures 5.3 to 5.5 present pertinent data relating to ice thickness, build-up rates and construction times for these islands.

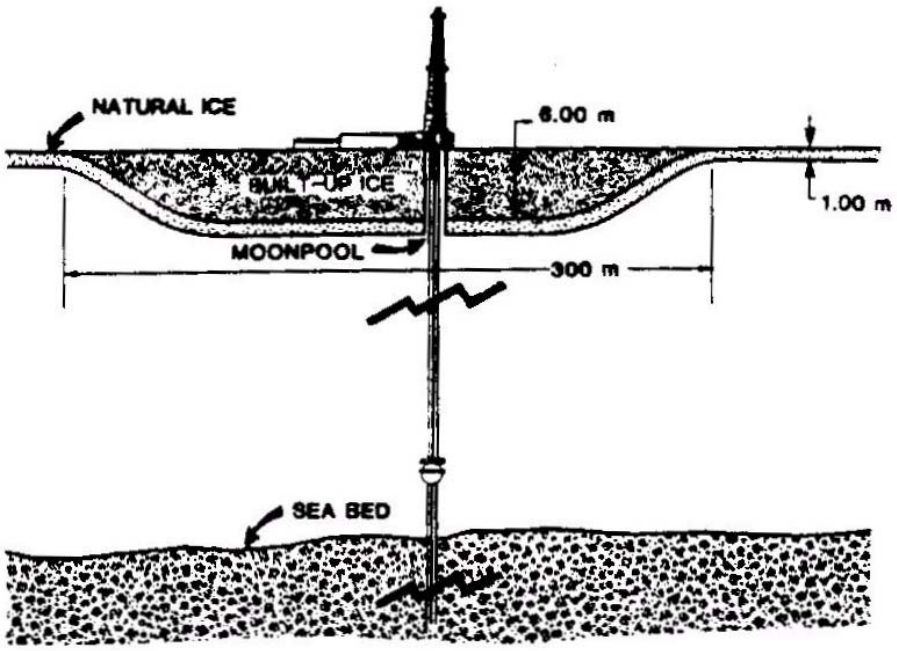

Figure 5.2: Cross-Section of Cape Alison Floating Spray Ice Island (Masterson et al, 1987)

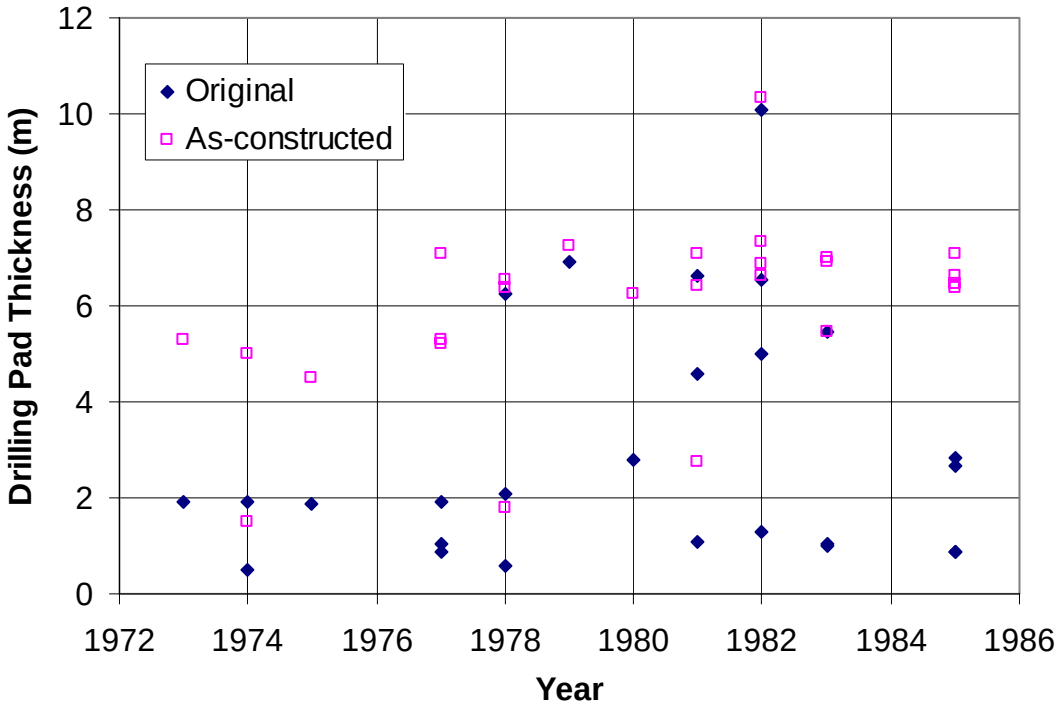

Figure 5.3: Ice Thickness Data for Floating Ice Islands

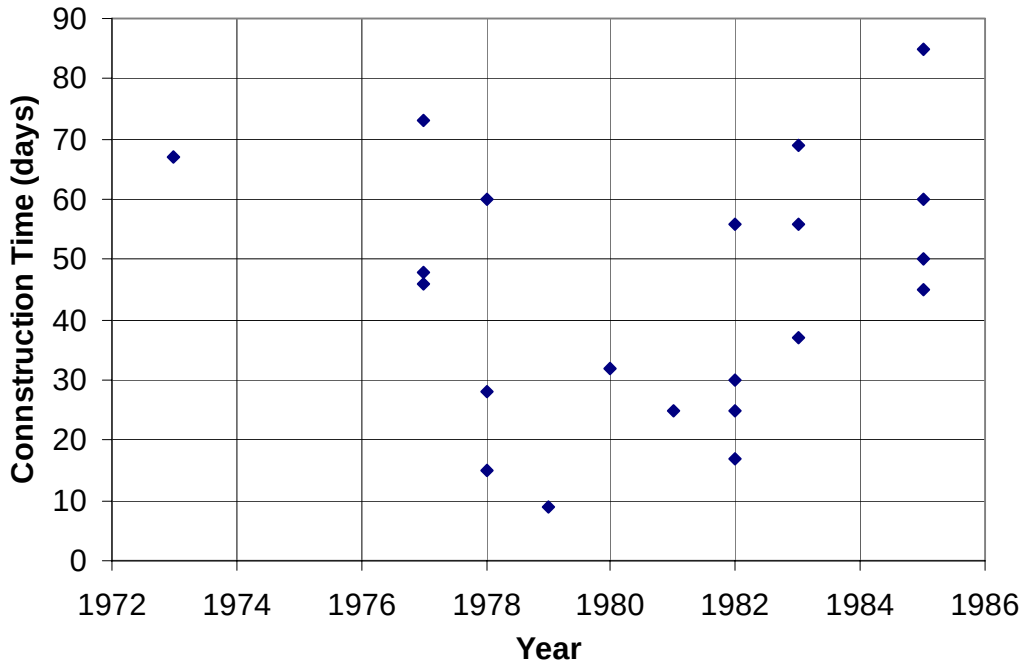

Figure 5.4: Construction Time for Floating Ice Islands

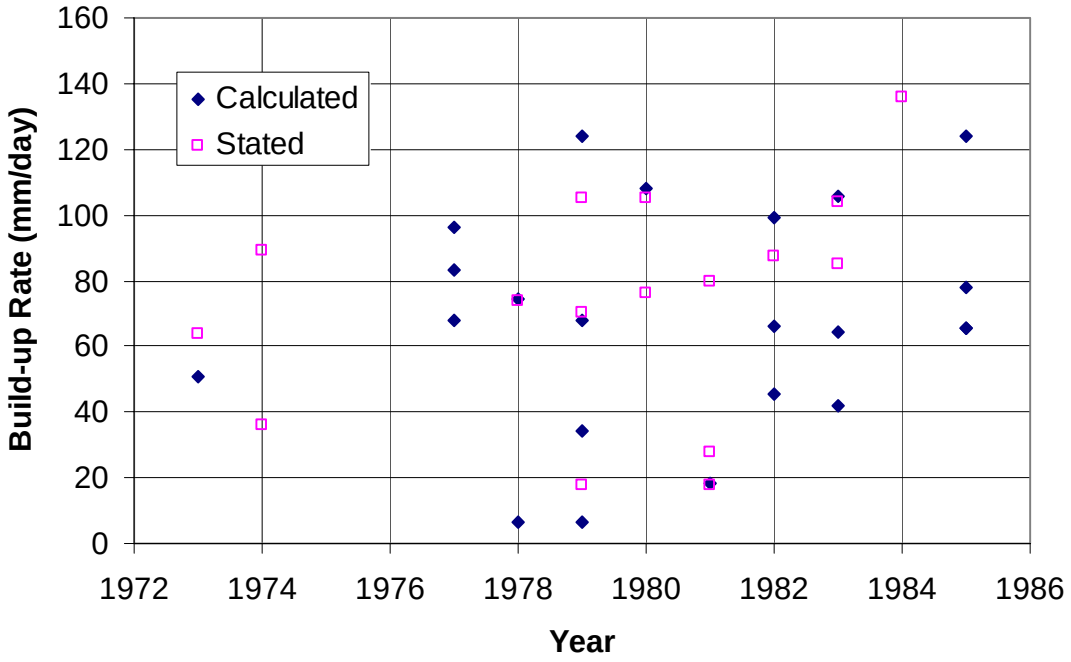

Figure 5.5: Build-up Rates for Floating Ice Islands

5.3 Grounded Ice Islands

Nearshore exploration drilling in the Beaufort Sea off Alaska and the Mackenzie Delta has a different requirement to that of the Canadian High Arctic. The flat seabed gradient in the nearshore area leads to shallow water depths at large distances offshore, and the ice movements are also potentially large. This large movement to water depth ratio makes drilling from floating ice unsuitable and the shallow water environment leads to the use of bottom-founded structures for use as drilling platforms.

Grounded ice islands are constructed in a similar way to floating islands, in that artificial ice is built up on top of the natural ice sheet to increase its thickness until it becomes grounded on the seabed. However, since the water column is shallow, any movement of the island in relation to the seabed will cause structural damage to the drill-string, and so the design requirement is to eliminate any differential movement. The island is therefore designed to withstand the horizontal force applied by the surrounding ice sheet by providing resistance through contact with the seabed. An additional requirement is to maintain the stability of the rig foundation, which will undergo creep settlement of the ice under loading.

As with floating platforms, start of construction is limited by the formation of stable ice and access to the drilling location. Generally to date, platform design has been performed using the natural ice to support equipment and personnel during construction. Access is

usually by ice road from a shore base, and so there must be sufficient ice thickness to support the construction and transportation loads. Landfast ice builds up in a stepwise fashion as onshore winds drive newly formed ice against existing ice to form stable grounded ridges. Landfast ice typically starts to form in October and can reach water depths of 18 to 25m by February (Weaver et al 1991). Experience shows that the ice is usually thick enough to start island construction during December. The duration of the construction period is highly variable, and depends on the volume of ice required to be formed, temperature and wind effects. Figure 5.6 shows the typical distribution of landfast ice in Harrison Bay, Alaska.

The first grounded ice island to be used for exploration drilling was constructed by Union Oil in Harrison Bay in 1977/78. It was grounded in 3m water depth using flooding techniques by applying thin layers of seawater to the ice surface and allowing to freeze in place. Generally, however, the relatively slow build-up rates achievable with flooded ice techniques limits the usefulness of these structures as grounded ice platforms. It is more suited to the construction of roads, which require less ice thickness.

The limitations of flooding as a construction technique was recognized, and a number of experimental programs were established to investigate alternative methods of forming ice islands. A major effort was undertaken by Exxon over a number of years in the 1970s to improve knowledge relating to spray ice design and construction issues, including the effects of deterioration during spring break-up. Field experiments began in 1979 and 1980 with the construction of a spray ice pads in the Canadian Beaufort Sea at Issagnak, and an island was also built in Harrison Bay, Alaska using three construction techniques: flooding, sprinkling and spraying (Kemp 1984, Reimnitz 1982). The Harrison Bay island, 400m in diameter, was grounded in 3.5m water depth to provide a final freeboard of 8m. The sprinkling system used an irrigation system, rotating around a central pivot to form the circular island. The use of high pressure, high volume pumps completed the island using spraying techniques. The island was monitored during the winter and subsequent break-up to assess the potential for maintaining an island through a summer season.

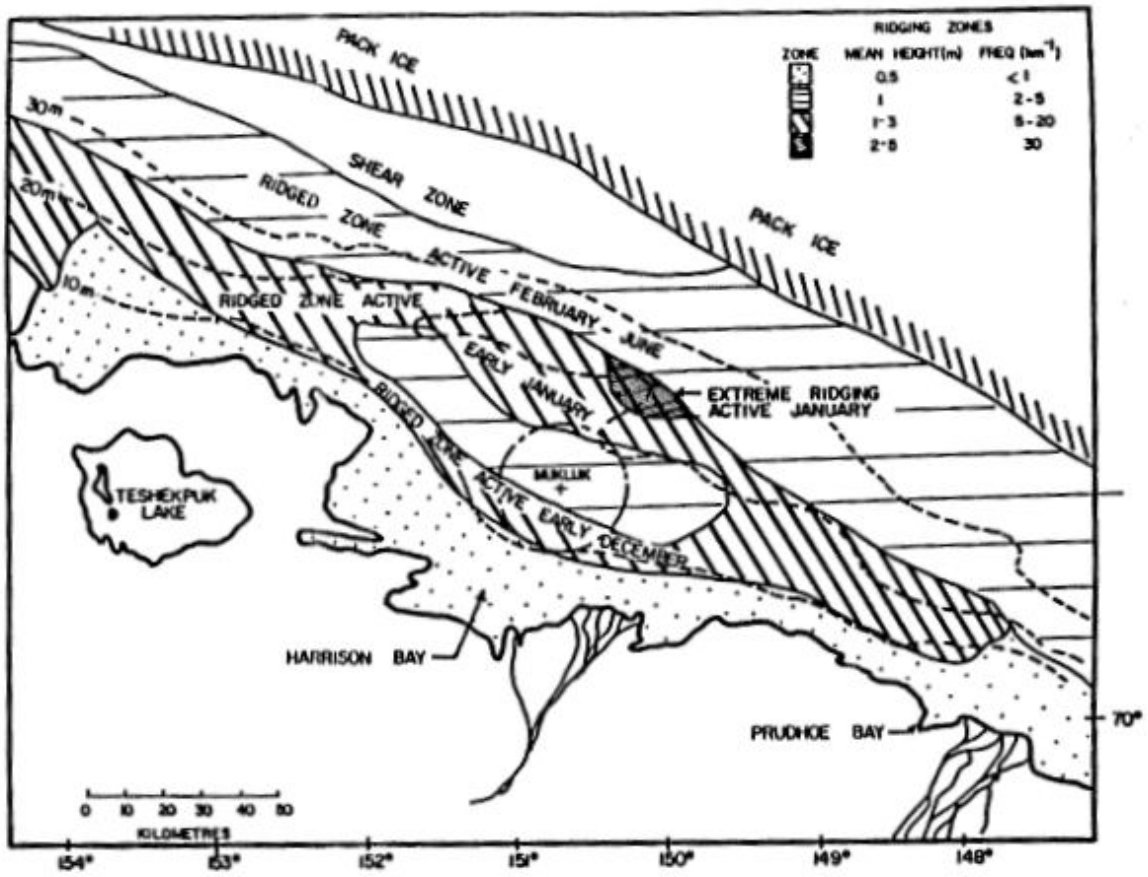

Figure 5.6: Landfast Ice Distribution in Harrison Bay, Alaska (O'Rourke 1984)

Further studies by Exxon and other operators led to the construction of a number of experimental spray ice islands to stabilise rubble fields and for potential use as relief drilling pads, such as at Tarsuit (Neth et al 1983), Alerk (Weaver 1997), Kadluk (Kemp et al 1988) and Isserk (Poplin & Weaver 1992). These islands were also used to study other properties such as ice forces and rubble formation. Figure 5.7 shows the Tarsuit relief pad built next to the main caisson retained drilling island.

The use of spray ice as a construction material for the formation of protection structures around drilling platforms was developed by Canmar, Sohio and Esso in the Canadian Beaufort Sea, using large capacity pumps mounted on the SSDC drilling structure and the Kigoriak ice breaker. The SSDC structure was placed onto a prepared sand berm and a number of spray techniques were used to supplement the rubble field that formed. Spraying using fire monitors allowed the efficiency of various systems to be assessed (O'Rourke 1984). This led to a number of protection structures being used under operational conditions to reduce ice loads on the CIDS bottom-founded platform. Figure 5.8 shows the principle of protection structure construction.

Figure 5.7: Tarsuit Relief Spray Ice Island (ICETECH, 2005)

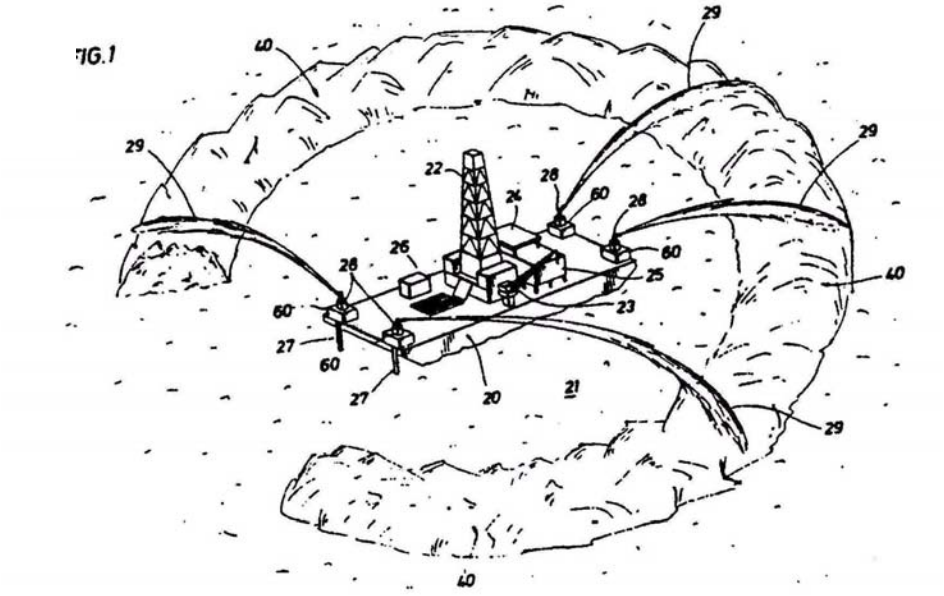

Figure 5.8: Principles of Spray Ice Protection Structure Construction (Finucane & Jahns, 1985)

The first use of an island built completely from spray ice for exploratory drilling was carried out by Amoco at Mars, Harrison Bay in 1986. This island was built on the landfast first year ice in 7.6m water depth, to provide a completed freeboard of 7.5m. The 330m diameter platform required 4 pumps to produce 1 million m^3 of ice during the 45 day construction program. Figure 5.9 shows the Mars ice island during drilling operations. The technical and financial success of this platform has led to spray ice becoming the material of choice for the construction of grounded platforms in shallow water in the Beaufort Sea. Construction cost savings of the order of 50% were quoted compared to sand and gravel islands previously used, as demonstrated in Figure 5.10. The construction of another 3 exploration spray ice islands in the 1980s at Angasak, Nipterk and Karluk reinforced the advantages of spray ice construction. Operational spray ice islands were used more recently at the Thetis Field in 2002/03, where a number of innovative techniques were successfully used by Pioneer Resources. This allowed the drilling of 2 wells using the same rig in the same season. A summary of grounded ice island construction is presented in Table 5.2, and graphical data relating to construction start dates, time to completion and build-up rates are given in Figures 5.11 to 5.13.

The development of ice island construction in the arctic has clearly shown that the use of spray ice provides substantial productivity advantages over flooding techniques. This report will therefore focus on spray ice as the method of choice for ice island construction.

Figure 5.9: Mars Spray Ice Island (MMS, 2005a)

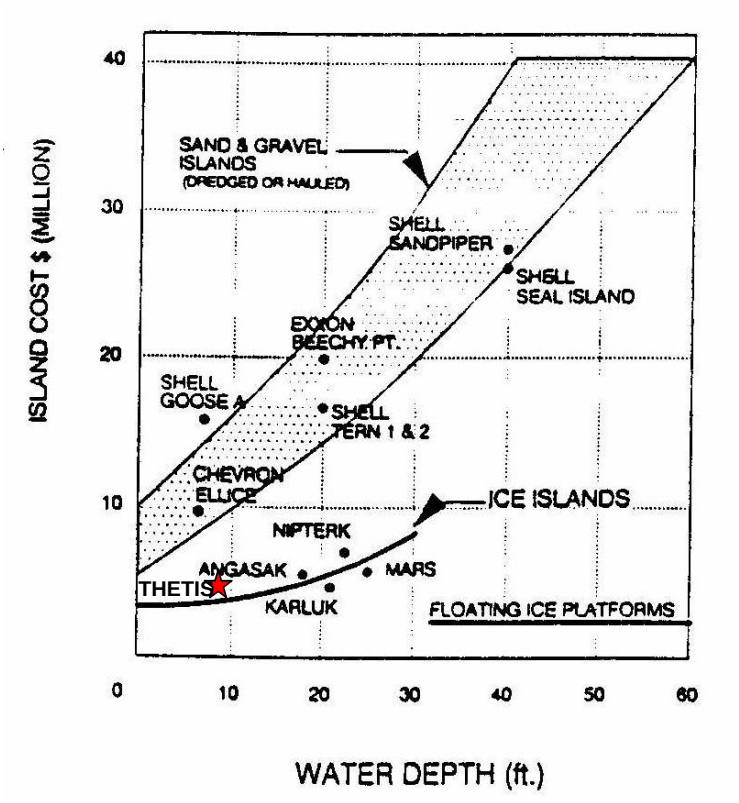

Figure 5.10: Cost Comparison Between Gravel and Ice Islands

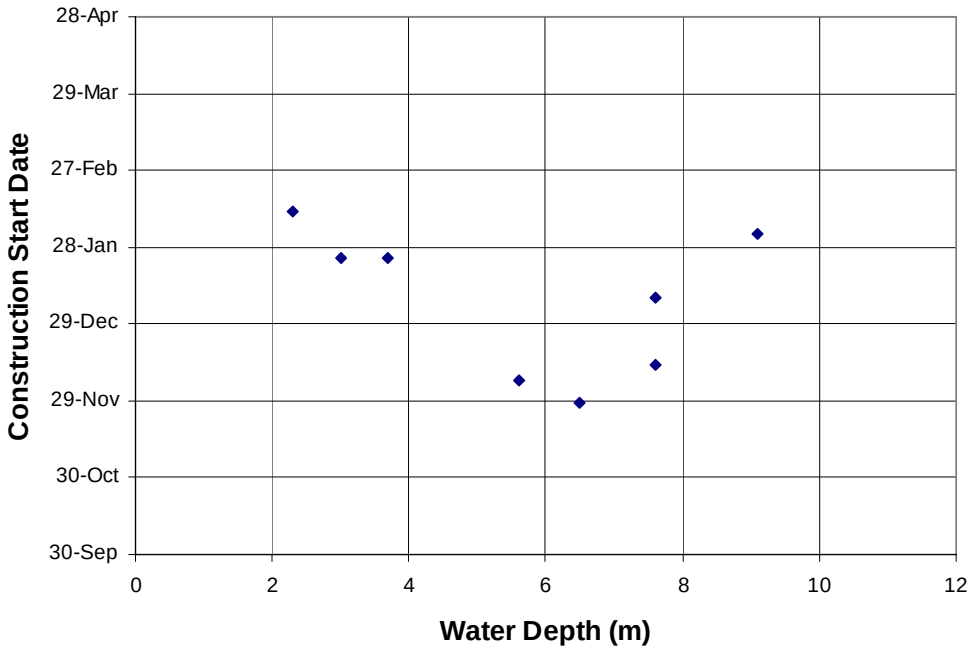

Figure 5.11: Starting Date of Construction for Grounded Ice Islands

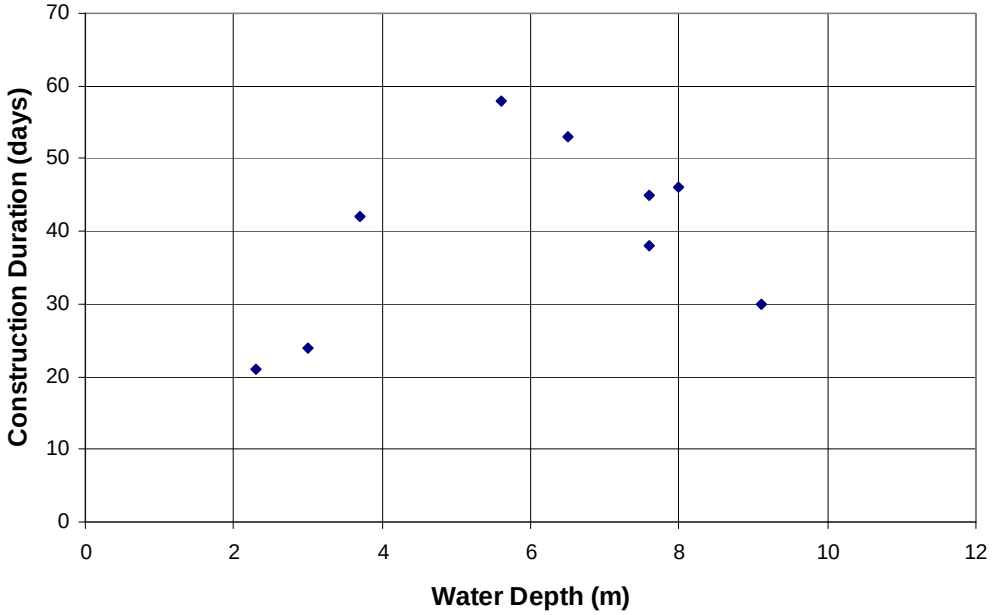

Figure 5.12: Construction Duration for Grounded Ice Islands

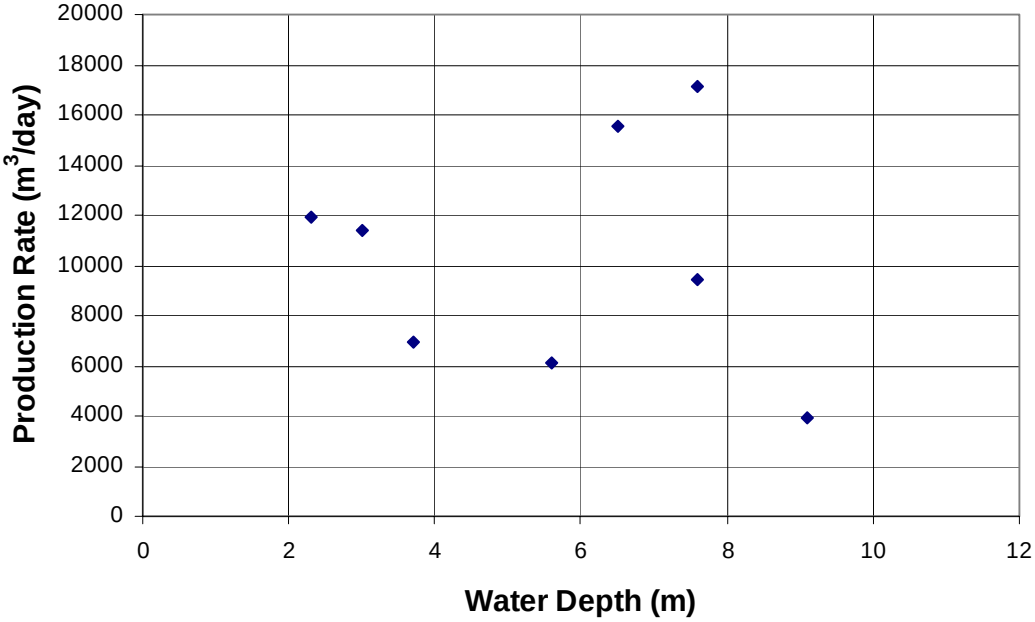

Figure 5.13: Production Rates for Grounded Spray Ice Islands

Table 5.2: Summary of Grounded Ice Pad Construction

Name	Operator	Location	Technique	Use	Dates	Water Depth
	Union Oil	Harrison Bay, US Beaufort Sea	Flood	Experimental Island	1977/80	3 m
	Exxon	Harrison Bay, US Beaufort Sea	Flood, Spray	Expermental Island	1979	3 m
	Esso	Canadian Beaufort Sea	Spray	Experiment	1980	
Tarsiut	Gulf Canada	Canadian Beaufort Sea	Spray	Relief Pad	1981/82	19.2 m
Alerk island	Esso	Canadian Beaufort	Spray	Relief Pad	1982	11.6 m
SSDC Uviluk	Canmar	Canadian Beaufort Sea	Spray	Experimetal Protection Structure	1982/83	30 m
Kadluk 0-07	Esso	Canadian Beaufort Sea	Spray	Relief Pad	1983/84	13.5
Sohio Rubble Generator	Sohio	McKinley Bay, Beaufort Sea	Spray	Experimetal Protection Structure	1983/84	13 m
Ice Island Experiment	Exxon	Canadian Beaufort Sea	Spray	Experimental Island	1983/84	13.7 m
Big Gun Expt., MV Kigoriak	Esso	McKinley Bay, Beaufort Sea	Spray	Experimetal Protection Structure	1983/84	14 m
SSDC Kogyuk	Canmar	McKinley Bay, Beaufort Sea	Spray	Experimetal Protection Structure	1983/84	28.4 m
CIDS Antares Barrier	Exxon	Alaskan Beaufort Sea	Spray	Operational Protection Structure	1984/85	14.9 m
Cape Alison C-47	Panarctic	Ellef Ringnes Island, Canadian Arctic	Spray	Operational Floating Island	1984/85	79 m
MARS full-scale prototype	Sohio	Harrison Bay, US Beaufort Sea	Spray	Experimental Island	1984/85	9.1 m
Mars	Amoco	Harrison Bay, US Beaufort Sea	Spray	Operational Island	1985/86	7.6 m
Angasak L-03	Imperial/Esso	Canadian Beaufort	Spray	Operational Island	1986/87	5.6 m
Nipterk P-32	Imperial	Canadian Beaufort	Spray	Operational Island	1988/89	6.9 m
Karluk	Chevron	US Beaufort	Spray	Operational Island	1988/89	7.6 m
Isserk I-15	Imperial	Canadian Beaufort Sea	Spray	Relief Pad	1989/90	11.5 m
Ivik	Pioneer	Thetis, Harrison Bay, Alaska	Spray	Operational Island	2002/03	3 m
Oooguruk	Pioneer	Thetis, Harrison Bay, Alaska	Spray	Operational Island	2002/03	3.7 m
Natchiq	Pioneer	Thetis, Harrison Bay, Alaska	Spray	Operational Island	2002/03	2.3 m
Kashagan, Sunkar Site	Agip KCO	North Caspian Sea	Spray	Operational Protection Structure	2002/03	
Kashagan, Aktote Site	Agip KCO	North Caspian Sea	Spray	Operational Protection Structure	2003/04	
Kashagan, Kairan Site	Agip KCO	North Caspian Sea	Spray	Operational Protection Structure	2003/04	

6.0 ICE PROPERTIES

6.1 Natural Ice Conditions

It is important to understand the Arctic ice environment prior to considering specific design or construction issues for ice islands, as this dominates the issues to be considered when operating in this region. Winter activities rely on sufficient ice thickness to support equipment, whilst also governing the loads applied to the resulting structures. Winter freeze-up and Spring break-up have important implications on schedules in terms of transport and longetivity of ice structures in open water.

Ice zones may conveniently be considered according to the following (Sanderson 1988):

6.1.1 Landfast Ice

Landfast ice forms adjacent to the north arctic coastline from October to May as freezing of the sea surface combines with accumulation of ice as it is driven by onshore winds. Movement is then largely prevented by attachment to the land and by grounded pressure ridges. Movements of up to a few metres can occur as a result of:

- Thermal expansion and contraction during the winter season, leading to the lowest displacements at the lowest strain rates;
- Wind driven movement which causes higher displacements of up to 10m at higher rates;
- Wind, combined with pack-ice push, which has the potential to cause very rapid and large movements up to 100m near the edge of the landfast ice.

Landfast ice reaches to approximately 20m water depth and has a maximum thickness of the order of 2m in April (Croasdale 1983), consisting of mainly first-year ice, although multi-year ice floes may be incorporated. Break-up of the landfast ice usually starts in May, leading to a mainly ice-free corridor between July and October.

First-year sea ice forms as air temperatures fall below zero degrees (0^{o}C) for sustained periods, starting in September. Level, relatively uniform, sheets of ice are formed under calm conditions and the heat transfer occurring during the formation of first-year ice is generally one dimensional upward heat movement through the ice cover and into the atmosphere (Frederking 1984). While Arctic seawater typically has a salinity of 30 parts per thousand (ppt), first-year sea ice salinity is generally around 5 ppt as a result of brine ejection during freezing. The salt content and grain structure of first-year ice influence its strength and failure behavior. Typically the upper 5 to 30 cm of the first-year ice cover is randomly oriented granular-grained structure while the remainder of the ice sheet is columnar-grained structure. Columnar grained ice crystals are oriented in a preferred direction, with the crystals elongated in the vertical direction. This produces ice that is

isotropic in the horizontal direction, but with different properties if loaded out of plane. Granular ice on the other hand, has similar properties in all directions.

Winds and currents initiate ice movements prior to complete freeze up, which can cause rafting or ridging of the first-year ice, resulting in larger ice formations. Rafting is common for ice less than 30cm in thickness, although sheets as thick as 2m have been observed to raft. Strong onshore winds also contribute to the growth of land-fast ice as newly formed ice is pushed against the existing land-fast ice sheet and help to form stable grounded ridges. The extent of this region is largely dependent upon the local water depth, prevailing wind direction, storm paths, currents, presence of islands and river outflows. Large ice ridges can result from compression or shearing action between the ice plates, with ridges up to 6 meters in height being common. Ridges become a dominant feature toward the edge of the land-fast zone from the 5 meter depth mark onwards. The grounding of these ridges contributes to the mechanism, which holds the land-fast ice in-place near the coastline.

6.1.2 Seasonal Ice – Shear Zone

This is a transitional, or shear zone, which exists between the landfast ice and polar pack. The width of this zone varies between a few kilometers and up to 300km within a season or year to year. The seasonal ice is relatively narrow and occurs close to the Alaskan shore due to the closer presence of the polar pack, whereas it is wider and further away from the Canadian Beaufort coastline. Seasonal ice is generally made up of first year ice, with some multi-year coverage.

Multi-year ice, is ice which has survived one or more melt seasons and tends to have much lower salinity as surface melt water produced throughout the course of a melt season, flushes a large amount of brine out of the ice. Salinity of less than 1 ppt is common above the waterline for multi-year ice, while 2 to 3 ppt is more common below the waterline. Multi-year ridges with extreme sail heights of 11 meters and keel depths of up to 31 meters have been observed within multi-year floes. The presence of multi-year ice in near shore regions promotes the development of early land-fast ice cover, with minimal ridging, which is vulnerable to sudden break-up (Derradji-Aouat et al 1991).

6.1.3 Polar Pack Ice

This refers to the permanent multi-year ice that occurs over the Arctic Sea Basins, which rotates clockwise with the Beaufort Gyre. In winter, it is surrounded by a matrix of first-year ice, and in summer leads open up as the pack edge melts back. Floes become detached from the pack and are capable of drifting into coastal waters during storms, causing hazard to offshore structures and shipping.

The circulation of the Arctic winds cause the ice-covered Arctic Basin to be in continuous motion, with ice movements up to a few kilometers a day, which causes a

great deal of shear deformation and mixing of first-year and multi-year ice. Almost the entire Arctic Basin ice cover is in continuous motion with the main areas being the Beaufort Gyre, Transpolar Drift, and East Greenland Drift.

6.1.4 Glacial Ice

Glacial ice originates on land from snow accumulation, compressed to sinter and entrap air voids within it (Frederking 1984). Glacial ice is observed either as icebergs, primarily on the east coast of Canada, and as tabular ice islands up to 10km in diameter and 30m thick in the Arctic Ocean. Glacial ice will not be considered in any more detail within this report.

6.2 Natural Ice Properties

Solid ice, representative of natural uncracked ice sheets, behaves as a visco-elastic material with strain rate dependent strength and deformation properties. A number of tests have been developed to provide quantitative parameters to describe ice behaviour, including fracture and creep. Field equipment suitable for determining ice parameters include the flatjack, borehole jack, pressuremeter, cone penetrometer, plate loading test, indentor and cantilever beam tests. Testing of laboratory samples of solid ice tends to be performed in uniaxial or triaxial apparatus. These tests may be performed under creep or fracture conditions, dependent on the rate of loading, and are used to determine stress-strain response of ice under specific conditions. The main aim in testing ice in the field or laboratory is to determine its bearing capacity and deformation characteristics under compressive, tensile or flexural loading. Of importance for ice island construction is the strength of the floating ice in flexure to allow support of vehicles and equipment, and its compressive strength as it applies lateral load to fixed structures. The force imparted by the ice sheet is limited by its strength and the mechanics of ice sheet failure are important in determining these values.

Ice strength is a function of ice type (first-year, multi-year, glacier), ice temperature, test geometry (including size effects) and test strain rate.

Flow creep theory of ice under long-term loading follows the following Equation 6.1:

$$\varepsilon_e = A\sigma^B t^C \qquad \text{(Equ. 6.1)}$$

Where: ε_e and σ_e are the equivalent Von Mises strain and stress
A, B and C are constants derived from creep tests and are temperature dependent
t is time

The effect of creep becomes important when considering the support of long-term loads on the ice sheet, particularly if they are sensitive to settlement effects such as a drilling rig.

A number of field programs have been undertaken to establish the properties of natural ice in the field (Sandwell 2003a). The Beaufort Sea Summer Ice Testing Project funded by the Arctic Petroleum Operators Association (APOA) in the 1970s provided a large amount of data on ice floes found within 80km of the coastline. Two phases, in July and September 1973 were aimed at determining the strength and stiffness of natural ice at different times of the season. A database of ice floe properties included position, size, thickness, strength, temperature, density and salinity.

Movement of the landfast ice sheet can occur relatively quickly and so short-term strength dominates the loading regime for most offshore ice-structure interactions. Appropriate values of load should also be derived using values related to size and aspect ratio of the interaction event. Temperature effects should be consistent with the measured temperature range for the time of year and region in question.

Further data on the effect of aspect ratio and initiation of other forms of failure are discussed in Section 7.

6.3 Spray Ice

Spray ice is formed by projecting water at high pressure into cold air. Heat transfer between the cold air and relatively warm water, coupled with the large surface area of the spray droplets, leads to the creation of ice crystals before the droplets reach the ground. Observations of spray ice production confirm that higher ice content is produced at lower temperatures, and that the process is largely ineffective at temperatures above –15^{o}C for normal sea water and efficient spray ice production occurs at temperatures colder that -20^{o}C (Jahns et al 1986, Bugno et al l990). The design of spray ice islands requires that it resists lateral loads imposed by movement of the natural ice, and that it provides adequate support for the drill rig and other equipment for the duration of the drilling program.

The proportion of ice formed from a water jet is a function of water droplet size, velocity, length of time the droplets are airborne and air temperature. A number of heat and mass transfer models have been developed that describe the formation of ice crystals from water spray (Allyn & Masterson 1989, Masterson 1992). A jet of water breaks into droplets as a result of inertial, aerodynamic and surface tension forces and the increased surface area promotes high rates of heat transfer between the water droplet and surrounding atmosphere. Depending on the position of any particular droplet within the spray, the water may nucleate before reaching the ground. The water droplet will be super-cooled during its travel from the spray nozzle, although the presence of a particle of sediment would aid nucleation. At this point latent heat is released and the water droplet temperature increases towards the freezing point as additional ice is formed at the freezing point (Szilder et al 1991).

The effect of salinity of the water spray, which is relevant for offshore ice island construction, was investigated by Sackinger et al (1978). The freezing process during

flight is not altered substantially, although the unfrozen content is made up of brine with a higher salinity concentration than the original seawater. The spray ice grains are deposited on the ground as fine sub-rounded granules of ice, which may partially bond to each other. On reaching the ground, the brine drains from the ice, resulting in an ice of lower salinity than the original seawater. The ice crystals also undergo sintering, in which the individual crystals bond together and increase in strength, effectively resulting in larger grain sizes.

The physics of spray ice formation is described in some detail in St. Lawrence et al (1992) and Steel (1989) and are not repeated in this report.

The engineering properties of spray ice are highly sensitive to density, temperature, salinity, degree of saturation, age and applied pressure. Spray ice is also a heterogeneous material due to the way it is formed, and samples produced under similar conditions would be expected to be layered and exhibit a large degree of variation.

The properties of spray ice under field conditions in the context of ice island construction can conveniently be separated into above-water and below-water ice. The principle properties of interest in ice island design are the mechanical strength, density and creep parameters of the ice. Other properties that would affect the above primary parameters include temperature, salinity and young's modulus, and these can be indicative of the variability of the primary parameters within an island. All of these properties should be routinely monitored to ensure the quality control of the spray ice structure.

As spray ice is deposited in layers above the water level during the build-up of an ice island, the unfrozen brine drains away relatively quickly and leaves a dry, partially bonded, material. As the overburden pressure increases due to build-up of the island, the ice density increases substantially. Even relatively unbonded slushy ice layers are transformed into bonded competent spray ice as a result of overburden pressure. The low ambient temperature required during spray ice formation results in a cold, and relatively strong material, exhibiting increasing density, strength and temperature with depth below the surface.

As a floating ice sheet is loaded by additional spray ice production, it will lower in the water and eventually ground on the seabed. As initially dry spray ice becomes submerged, it will become saturated with seawater and quickly adopt thermal equilibrium with the surrounding seawater at a temperature of -1.8^{o}C. Saturation of the pore space results in a reduction in grain-to-grain contact forces and therefore results in a lower strength. In addition, buoyancy forces acting on the underwater ice leads to a reduction of vertical stress with depth below water level.

6.3.1 Spray Ice Strength

A number of field and laboratory tests are used to determine spray ice strength. In-situ techniques include the use of flat jacks, pressure meters and cone penetrometers. Laboratory tests usually consist of triaxial tests performed in temperature controlled coldroom conditions. The stress-strain properties of spray ice suggests that it is a strain-hardening material, exhibiting a bilinear loading behaviour as shown in Figure 6.1. Measured strength is a function of temperature, density, strain rate, confining pressure, consolidation time and pressure and test method, and so cannot be presented as a single number.

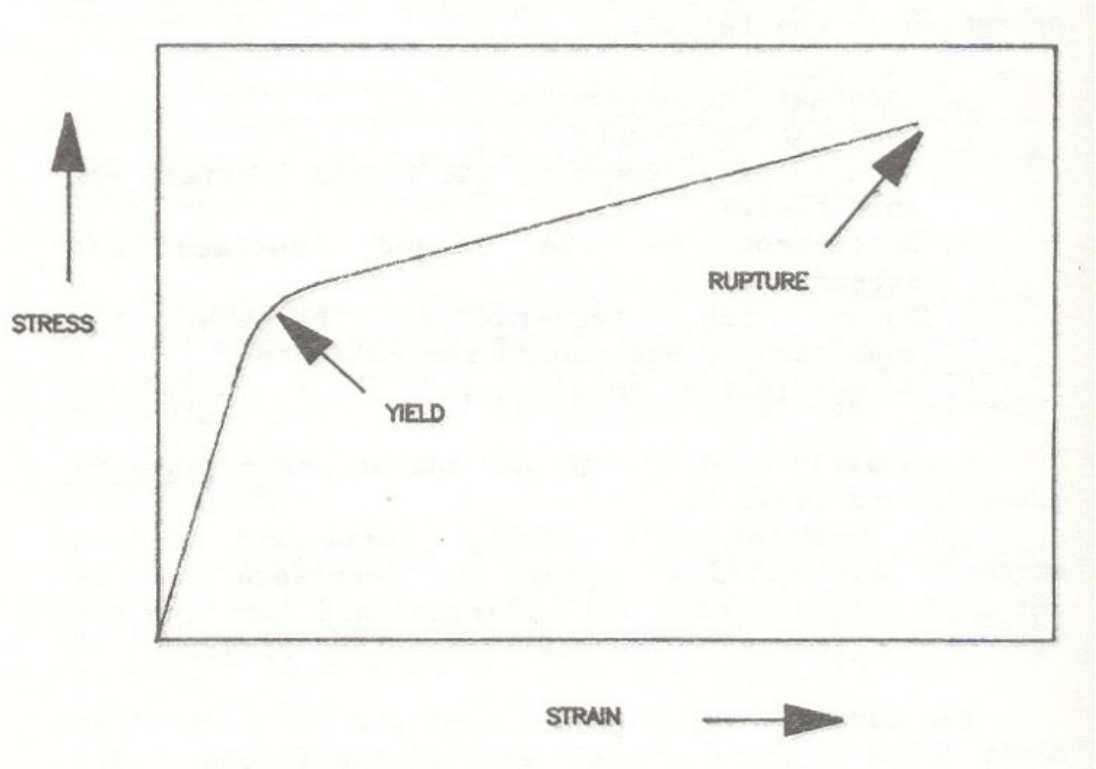

Figure 6.1: Typical Stress-Strain Behaviour of Spray Ice (Weaver et al 1988)

Steel (1989) undertook a comprehensive program of triaial testing of laboratory produced dry spray ice under a range of conditions. The strain rate was large enough that creep is not considered to be a significant factor in the results. Typical results are given in Figures 6.2 to 6.5, to demonstrate the effect of consolidation time, confining pressure, strain rate and temperature. These results highlight the importance of understanding the conditions under which the spray ice is tested to ensure that they are representative of actual field conditions.

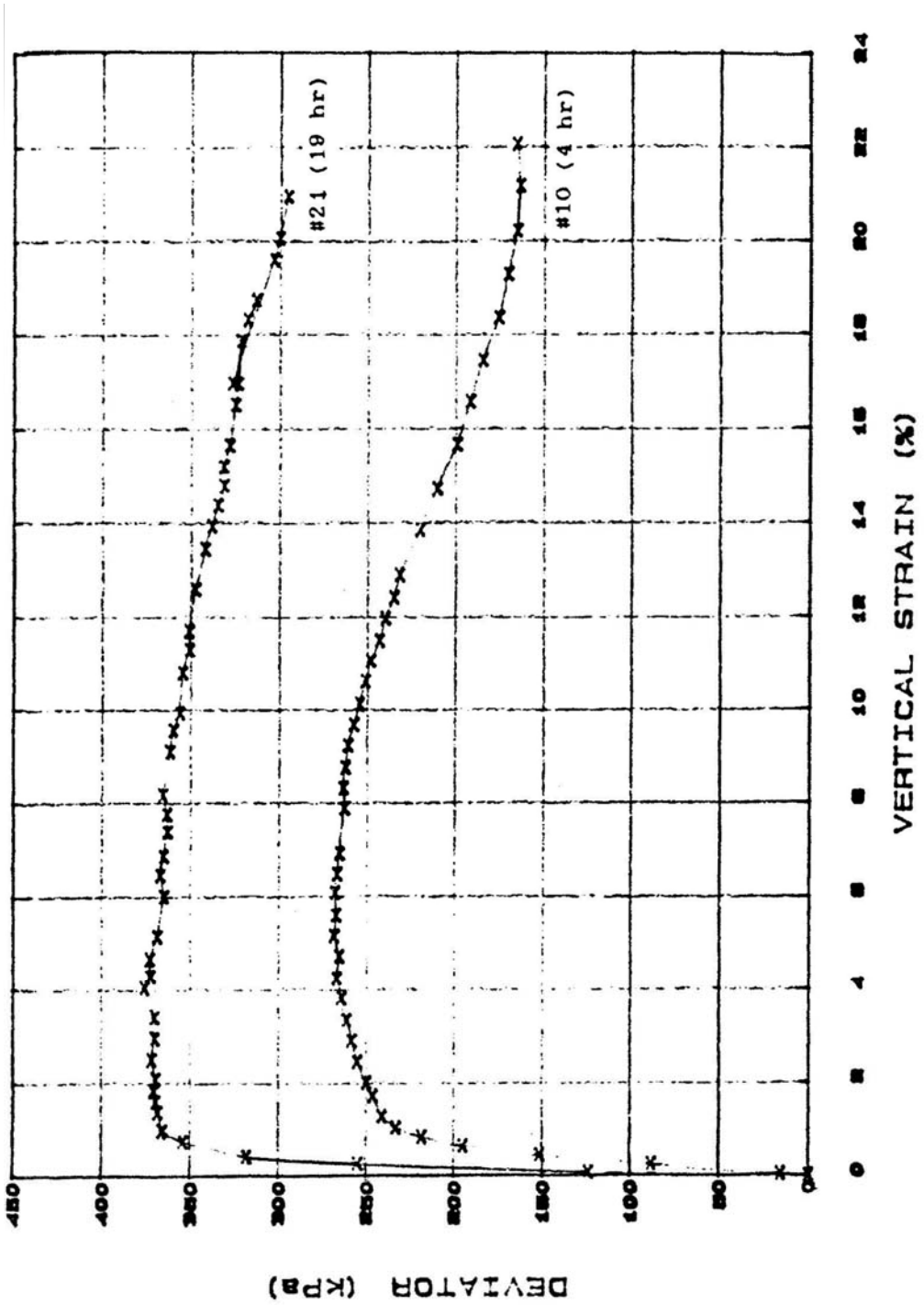

Figure 6.2: Stress-Strain Behaviour of Spray Ice as a Function of Consolidation Time (Steel 1989)

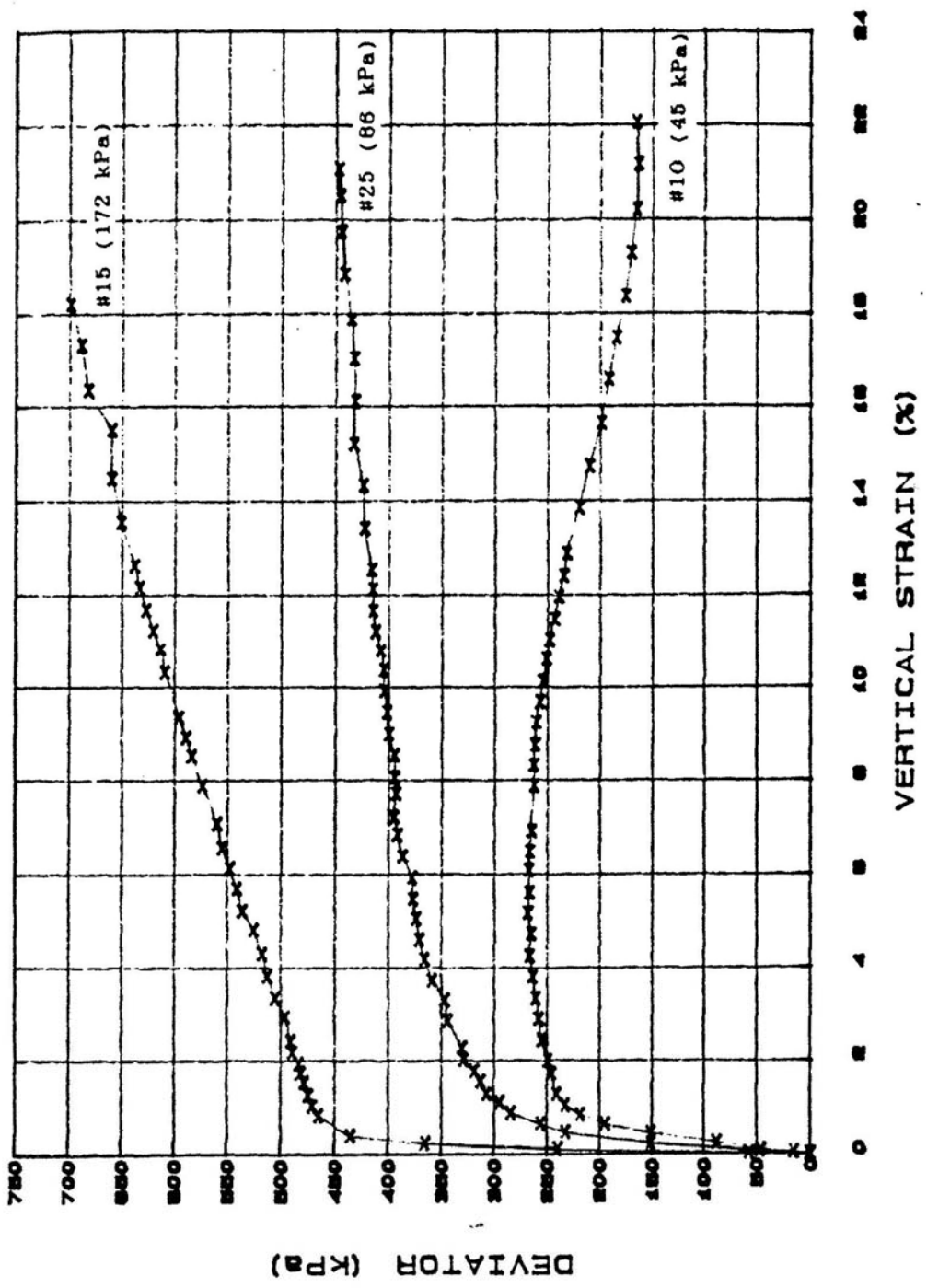

Figure 6.3: Stress-Strain Behaviour of Spray Ice as a Function of Confining Pressure (Steel 1989)

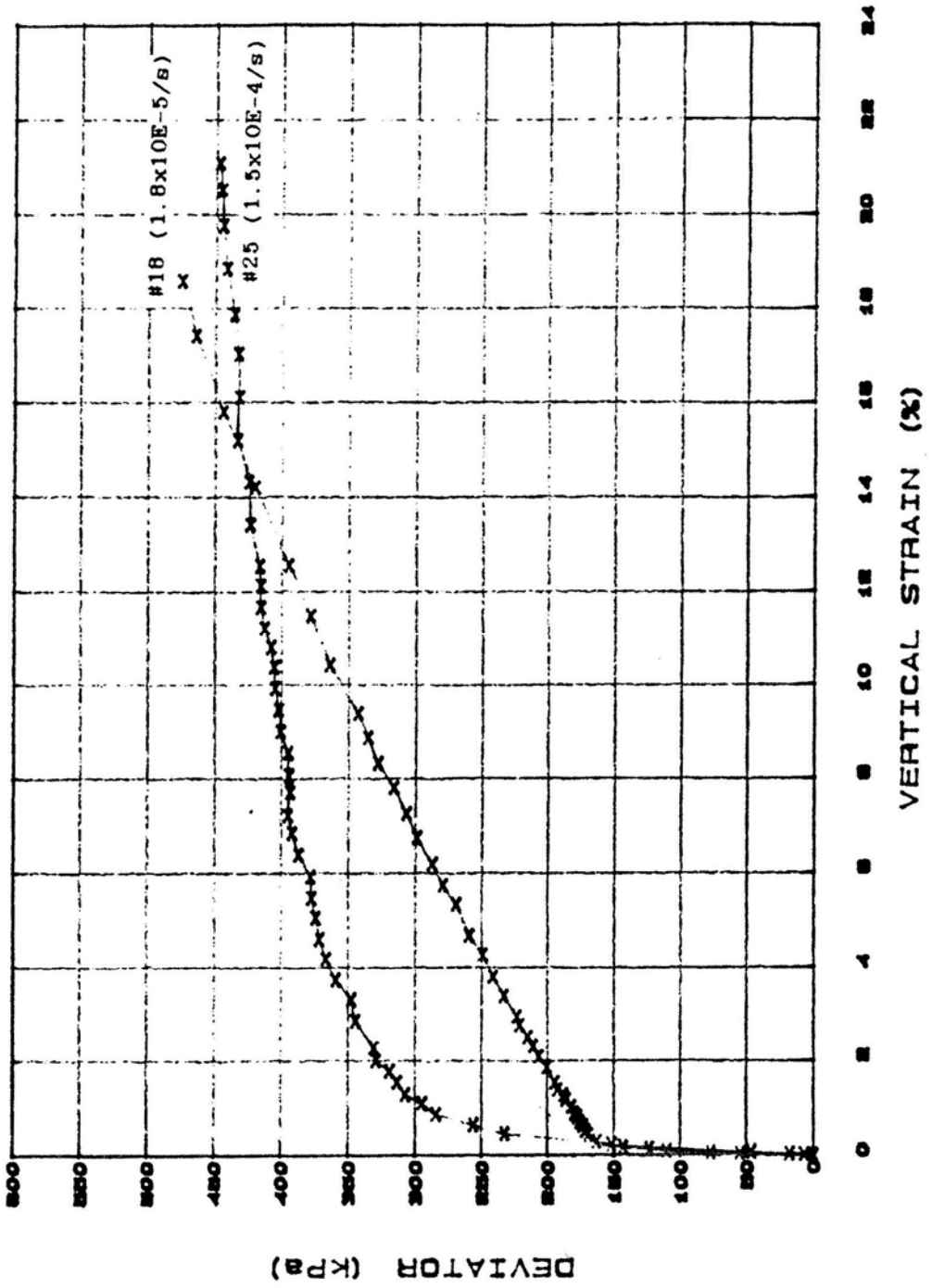

Figure 6.4: Stress-Strain Behaviour of Spray Ice as a Function of Strain Rate (Steel 1989)

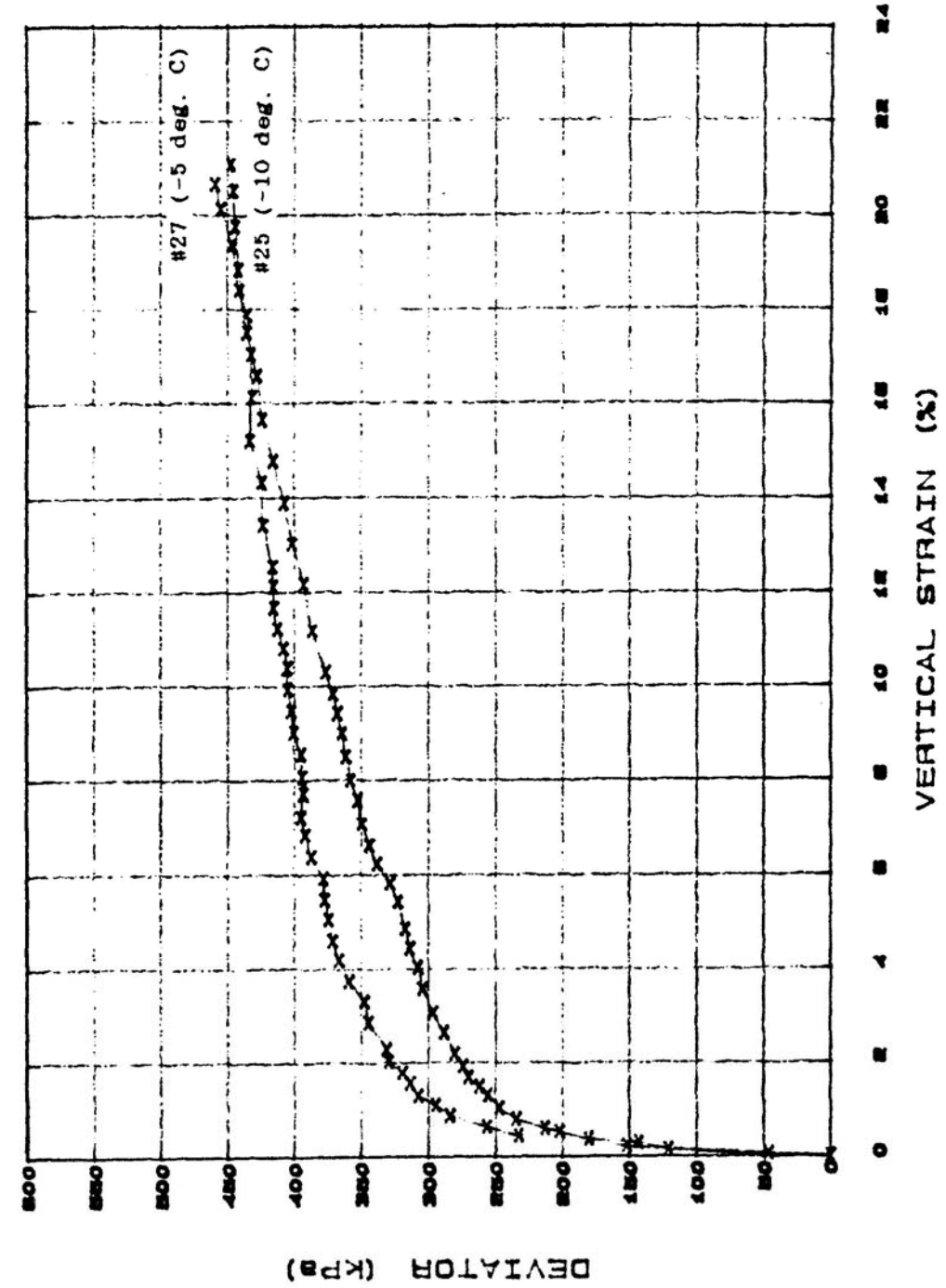

Figure 6.5: Stress-Strain Behaviour of Spray Ice as a Function of Temperature (Steel 1989)

The results of the triaxial tests indicate that adopting Mohr-Coulomb failure criteria adequately represents the results for the range of conditions tested, although the actual failure mechanism may not be completely consistent with this theory. The Mohr-Coulomb failure criterion takes the form of Equation 6.2:

$$\tau = c + \sigma \tan\phi \qquad \text{(Equ 6.2)}$$

Where τ is the shear stress developed along the failure plane, c is the cohesion intercept, σ is the normal stress acting on the failure plane, and ϕ is the angle of internal friction of the material.

A cohesion, c of 70kPa and internal angle of friction, ϕ of 28^o were back-calculated from the Steel (1989) tests as shown using a Mohr-Coulomb plot in Figure 6.6. A curved failure surface is also shown, which may be more representative of the test results. Figure 6.7 presents the data for all test samples in terms of strength and confining pressure for direct use in design. The definition of failure strength is also subjective for a strain-hardening material, and the strain at which failure occurs should be consistent between data sets. This dataset considers the strength at the point of "turnover" on the bilinear stress-strain plot (the point of sudden change in gradient on the stress-strain curve), which occurs at approximately 0.2 to 0.5% strain. This corresponds well with the Imperial Failure Model described in St. Lawrence et al (1992), although a curve-fitted model was developed to provide a strength equation that depends on material constant, strain rate and temperature.

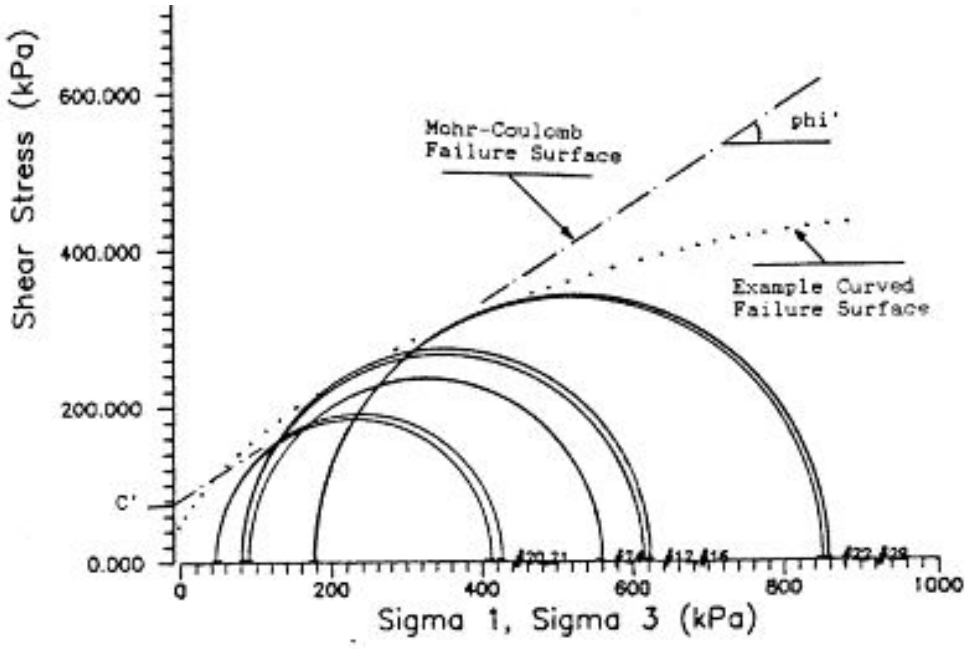

Figure 6.6: Mohr-Coulomb Failure Criterion for Triaxial Test Results (Steel 1989)

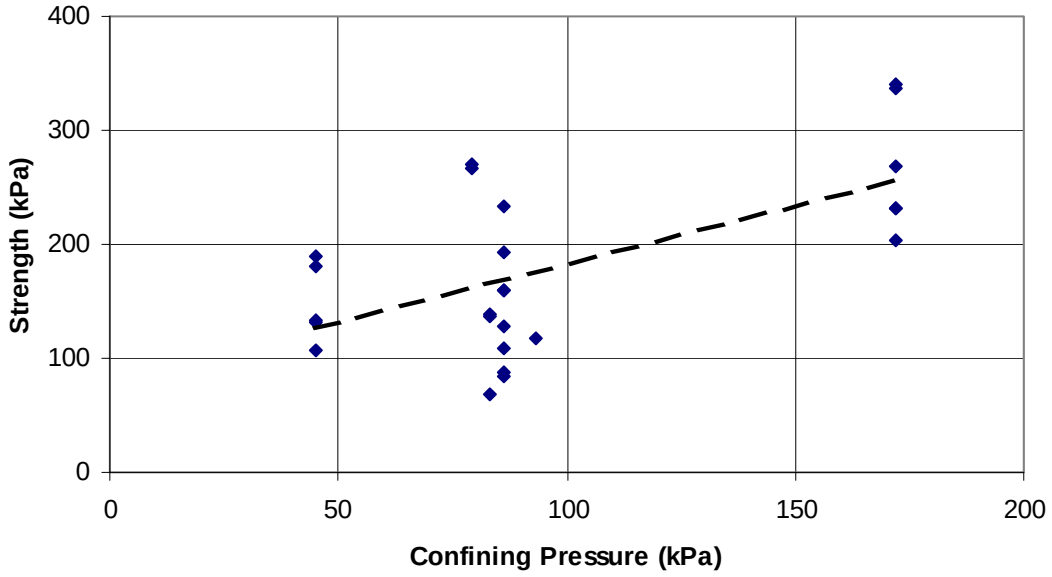

Figure 6.7: Triaxial Test Results for All Samples (Data from Steel, 1989)

By contrast, the Thetis ice island design report (Sandwell 2003b, Masterson et al 2004) used a spray ice strength of 280kPa cohesion, 0.85° internal angle of friction based on data from previously constructed islands. Chen & Gram (1989) suggest values of 11.5kPa and 51.5° respectively.

Saturated spray ice is more difficult to sample from under-water locations and to perform strength tests than above water ice. In general, strength is obtained from in-situ tests such as pressuremeters, flatjacks and cone penetrometers. It is considered that Mohr-Coulomb failure criteria may not be as applicable for saturated spray ice in a relatively warm environment, and that a stress independent parameter should be used, analogous to undrained shear strength in clay soils. However, a review of results obtained from a number of sources suggests a wide variance in values as demonstrated in Table 6.1.

The data provided in Table 6.1 has been used to determine the variation of shear strength with depth through a typical island is given in Figure 6.8. A freeboard of 6m in a water depth of 6m has been used for illustrative purposes. This demonstrates the uncertainty in determining the strength of spray ice islands for use in design and the resulting wide range of design parameters that can result.

Table 6.1: Summary of Spray Ice Strength Used in Design

Author	Above Water Strength		Below Water Strength	
	Cohesion (kPa)	Friction (deg)	Cohesion (kPa)	Friction (deg)
Steel (1989)	70	28		
Chen & Gram (1989)	11.5	51.5	11.5	51.5
Imperial Model (St Lawrence 1992)	160	-	80	-
Karluk Design (St Lawrence 1992)	146	-	19	30
Thetis Design (Sandwell 2003b)	282	0.85	40	-
Nipterk Design (Weaver & Poplin 1997)	150		68	
Previous Data (Sandwell 2003b)			40 to 217	

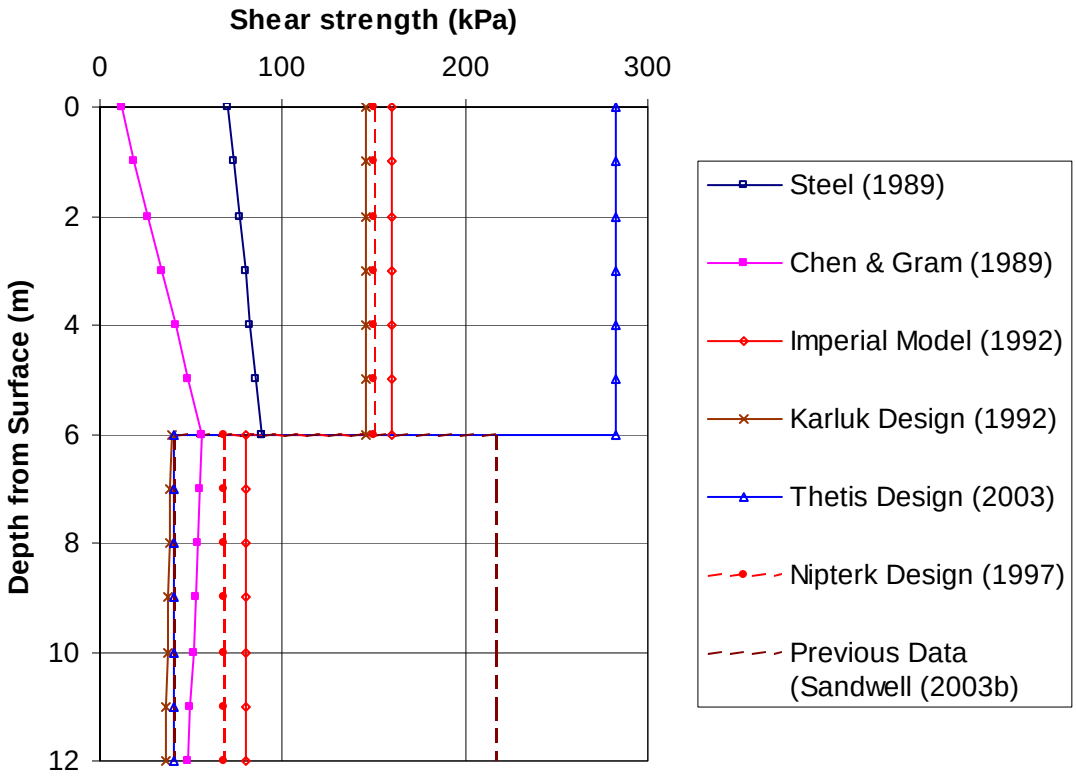

Figure 6.8: Variation in Design Strength Parameters for Typical Ice Island

A review of the design criteria used in practice for spray ice islands suggests that the strength of the island itself is rarely critical in determining resistance to lateral ice loads, but rather the sliding shear developed between the island and the seafloor. The general practice has therefore been to adopt a safe, lowerbound strength profile and undertake a check that it is adequate.

6.3.2 Spray Ice Density

The density of spray ice is important in determining its shear strength, which is a function of overburden in a number of models as discussed in Section 6.3.1. Density also determines the ground bearing pressure of the island on the seabed, which will determine the sliding resistance on sandy soils.

The density of dry spray ice is easily defined as the weight of a known volume of ice crystals, and is directly related to the porosity of the sample being measured, depending on the level of compaction or consolidation. The results of a large number of tests on in-situ and laboratory prepared samples suggests that density of dry spray ice is in the range of 600 to 750kg/m^3. The dependence of measured density on confining load and its

natural variability are demonstrated in Figure 6.9 using data from the Steel (1989) triaxial test data on dry spray ice. Density data from Sandwell (2003b) for the Thetis ice islands shows that slightly lower density measurements are achieved under field conditions as shown in Figure 6.10, and the relationship of increasing density with confining pressure (depth) is evident.

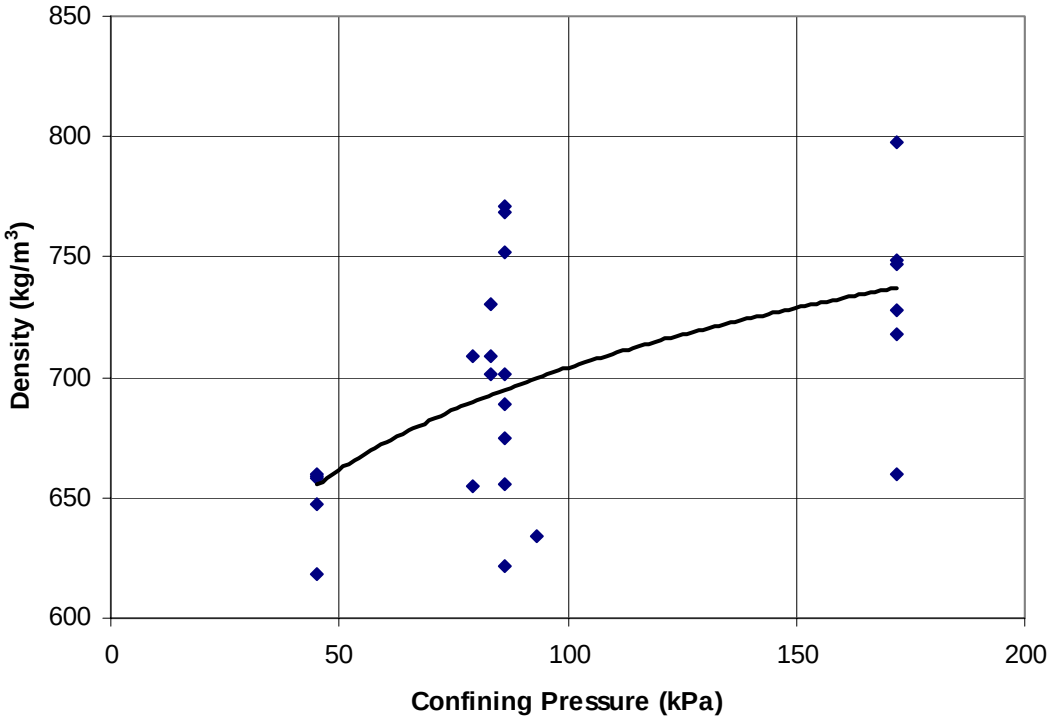

Figure 6.9: Variation of Density with Confining Pressure from Triaxial Tests (Data from Steel, 1989)

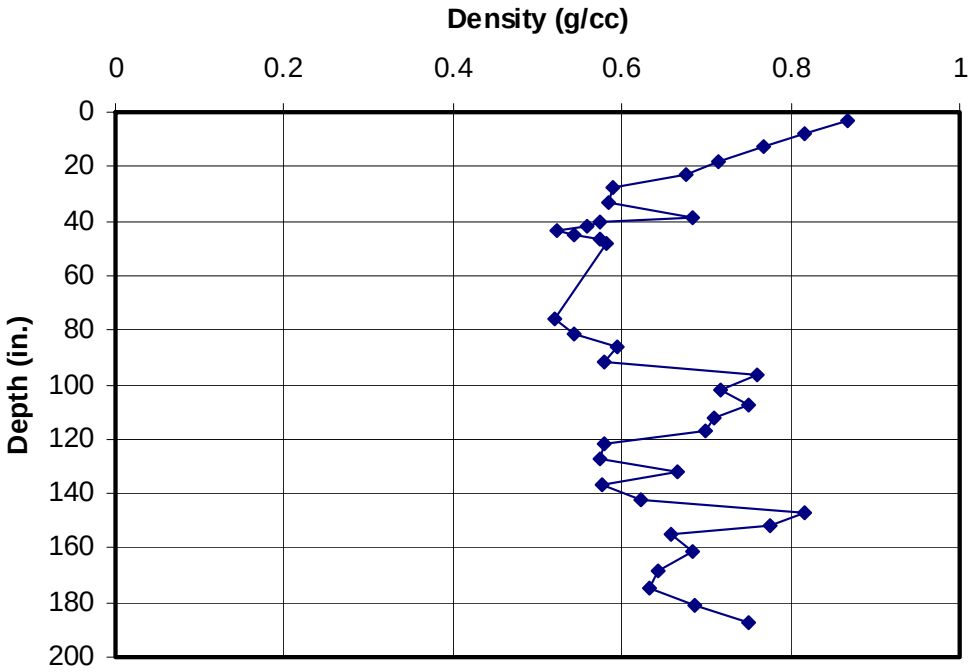

Figure 6.10: Measured Density Profile at Thetis Ice Islands (Sandwell, 2003b)

Submerged spray ice has its pore space saturated with water (seawater in ocean environments), and is more difficult to measure directly. It should be noted that submerged spray ice is not necessarily completely saturated and may contain some trapped air. It may be defined in the same way as dry spray ice, by including the weight of the water within the pores, or in terms of a buoyant weight, which would be negative and also be a function of the density of the surrounding water, which would in turn depend on its salinity. Typical under water buoyant spray ice densities are in the range of –90 to –120 kg/m^3 (St Lawrence 1992).

6.3.3 Spray Ice Creep

The creep properties of spray ice for use as a drilling support base are important in determining the expected settlement of drilling rigs and other facilities supported on the island. A spray ice island undergoes creep initially during and immediately after construction due to increased overburden pressure. This is then followed by creep settlement under the applied load of heavy equipment such as drilling rig, storage facilities and accommodation modules. Further surface settlement late in the winter season would also be expected due to melting as warmer weather develops. The drilling rig, in particular is sensitive to settlement during drilling operations and acceptable settlements are in the region of a few hundred millimetres. It has been noted that spray ice, due to its low density and open structure undergoes creep at a rate of up to 100 times that of solid columnar ice (Shields et al 1989).

Power law creep follows the same principles as described for natural ice, where creep rates are a function of some exponent of applied stress and temperature. Creep tests are performed in-situ using pressuremeter testing, or in the laboratory using stress-controlled loading apparatus. In-situ techniques are preferred as they do not subject the ice to as much disturbance and can be performed under more realistic conditions.

A large number of creep tests have been performed on spray ice islands to determine the long-term deformation behavior of spray ice. Test durations of 30 to 100 days on Nipterk Island (Weaver & Poplin 1997) determined that creep rates converged to a strain rate of about 0.0005/day after 50 days of loading under those particular test conditions. Vinogradov and Masterson (1989) developed an analytical model for predicting the creep response of spray ice islands under self weight and rig loading. A summary of recorded creep on spray ice structures (islands and barriers) is given in Table 6.2, indicating that average creep rates of the order of 2 to $5x10^{-9}$/sec (per second) provide a good basis for design.

Table 6.2: Interpreted Creep Rates from Ice Island Structures (St Lawrence 1992)

Structure	Total Creep Settlement	% Strain	Overall Creep
Mars	1.74m / 33 days	1.14	$4*10^{-9}$ /sec
Angasak	0.175m / 74 days	1.5	$2.3*10^{-9}$ /sec
Nipterk	0.21m / 112 days	1.9	$2*10^{-9}$ /sec
Karluk	0.127m / 33 days	0.9	$3.2*10^{-9}$ /sec
CIDS Antares Barrier	0.61 - 0.76 m / mth (1st 2 months)	1.8 /mth	$3.4 - 8.5*10^{-9}$ /sec
Orion Experiment	0.67m / 61 days	2.3	$4.4 - 5.5*10^{-9}$ /sec

Since creep settlement is highly sensitive to ice temperature, it is important to maintain and control this parameter. One area in which heat transfer and potential warming of the ice is through the use of drilling muds, particularly during the return cycle. Systems have been developed to provide insulation and active cooling of the well cellar in an effort to maintain cold ice temperature to prevent excessive settlement or outright thawing. Adequate insulation in the vicinity of all heat sources, eg. accommodation units is also important during operations.

7.0 DESIGN

7.1 Floating Islands

Design of the floating islands typical of those constructed in the Canadian High Arctic was based on the theory of elastic plates resting on an elastic foundation. The platforms were constructed on stable ice such that lateral ice movement was not a concern. The following equations (Sandwell 2003a) were adopted for calculating maximum loads and deflections:

$$\sigma_{max} = 0.275(1+\upsilon)(P/h_i^2)\log(Eh_i^3/kb^4) \quad \text{(Equ. 7.1)}$$

$$\delta = P/8kl^2 \quad \text{(Equ. 7.2)}$$

$$\text{with } l = (E^*h_i^3/12(1-\upsilon^2)k)^{1/4} \quad \text{(Equ. 7.3)}$$

Where: σ_{max} is the maximum fibre stress, υ is Poisson's ratio of the ice sheet, P is the applied load, h_i is the ice thickness, E is the elastic modulus of the ice sheet, k is the unit weight of water, b is the loading radius, δ is the calculated deflection, l is the stiffness length given by Equation 7.3 and E^* is the longterm elastic modulus given as 0.1E to allow for creep behaviour. A typical value of elastic modulus used for the Panarctic islands was 5.5GPa (10^6 kPa), although the specific conditions of the ice at the location of interest should be used in design.

Typical values of safe fibre stress used in the floating platforms are σ_{max} of 520kPa and deflection, δ equal to the freeboard of the floating island. These are unfactored values, which should be adjusted to include an appropriate factor of safety. The required design ice thickness for the Panarctic floating islands was approximately 5 to 7m, to support a typical 1300 to 1600 tonne rig weight.

7.2 Grounded Islands

The primary design consideration for a grounded ice island is to provide adequate lateral stability to overcome loads imposed by the natural ice sheet. Such loads in nearshore landfast ice are primarily due to thermal expansion forces generated during temperature changes and are restricted to relatively small movements of the order of metres within one season. Island locations further from the coastline and closer to the shear zone can be subject to landfast ice "breakouts". In these events, the ice can be moved up to 100m, usually during storms with offshore winds. Such events are rare, but require ice loads to be calculated for high strain rates. Experience of grounded ice island construction is currently limited to landfast ice, and discussion in this section will be based design criteria for this case. The construction of spray ice protection barriers in shear zone ice conditions, however, does provide experience for design under such scenarios. Further, the use of spray ice islands for drilling in the shear zone is also being considered.

7.2.1 Ice Loads

The ice load applied to a structure is usually calculated by considering the lower of the driving force or the failure load of the ice sheet or structure. In the case of landfast ice undergoing thermal expansion or sudden shifts due to storm events, the driving force can be considered infinite and the process will be dominated by the local failure load at the island. Failure can be defined within the ice sheet or within the island. In undertaking design calculations, it is required that the load capacity of the island is greater than the ice failure load by an appropriate factor of safety.

The primary design criterion of an ice island should be its ability to withstand the forces exerted on it by movement of the surrounding ice sheet. Factors influencing the expected magnitude of the forces include; ice island location, level ice thickness, net seasonal movement, air and ice temperature and ice velocity.

The total force that must be resisted by the ice island will depend on the failure mode of the ice at the interface with the island.

Two possible failure modes should be considered:

- Crushing of the surrounding level ice as it moves against the island;
- Passive failure of the edge of the spray ice island (at a lower load than the level ice out-of-plane failure). This would be followed by out-of-plane failure of the advancing level ice.

These failure modes are shown and (a) and (b) in Figure 7.1.

The global resistance of the island is required to be greater than the ice loads derived according to the above mechanisms. Global failure of the ice island should be checked for the following:

- Sliding along the sea floor;
- Shear failure through the ice island core just above the seabed as shown in Figure 7.1 (c).

It should be noted that Figure 7.1 is drawn with an exaggerated vertical scale of approximately 5 times.

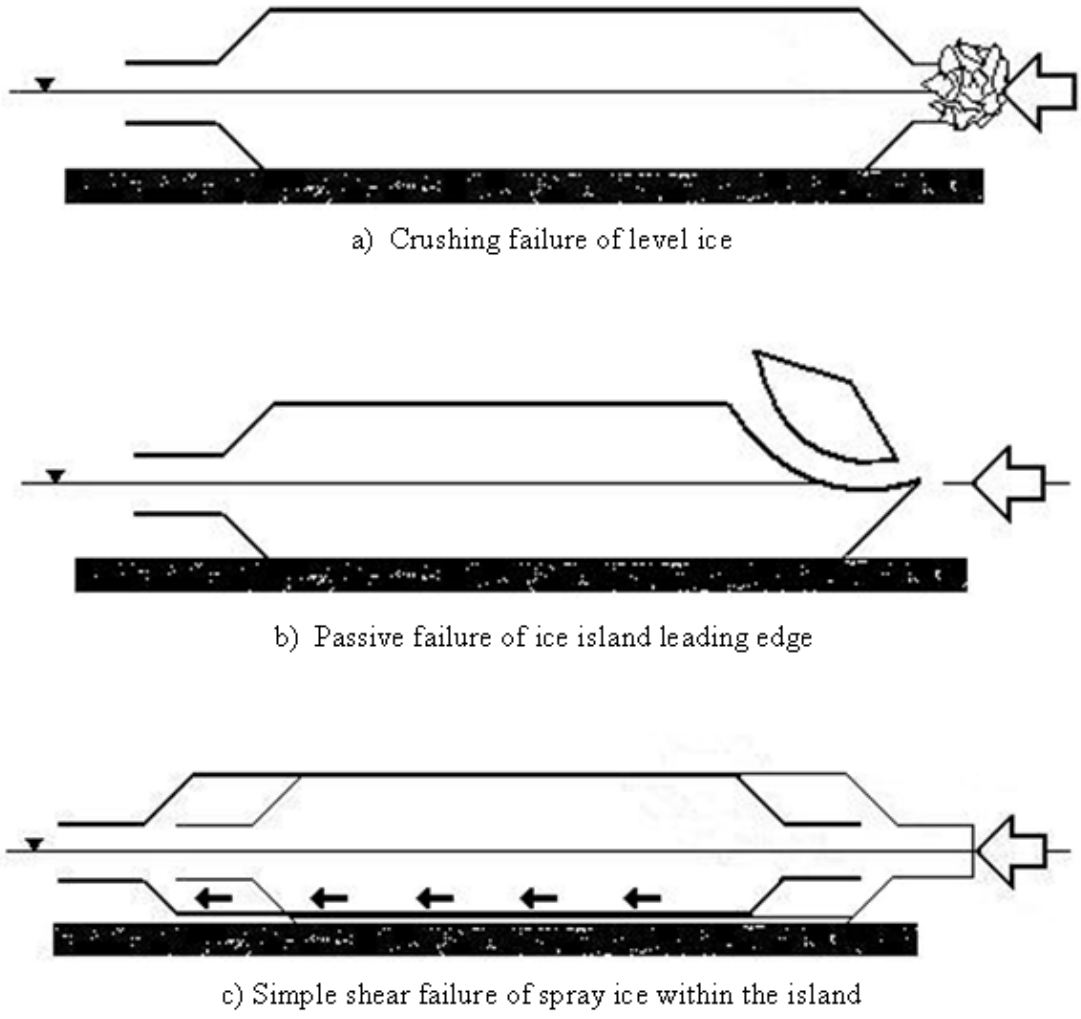

Figure 7.1: Potential Failure Modes for Spray Ice Island (St Lawrence 1992, modified)

7.2.2 Crushing failure of level ice

The crushing failure of level ice per unit width, F_c, is the product of effective ice pressure, p_{eff}, and ice thickness, h_i:

$$F_c = p_{eff} h_i \qquad \text{(Equ 7.4)}$$

Equation 7.4 represents the limiting upper bound force that can be applied to the island. Sandwell (2003b) based their effective ice pressure on the results of "Joint Industry Project Beaufort and Chukchi Sea Arctic Production Platforms - Update" (Sandwell, 1999), and presented in Masterson and Spencer (2000). Figure 7.2 contains this ice pressure as a function of thickness that allows calculation of the global ice load on wide structures. For typical design ice thicknesses in the Beaufort Sea, a global ice pressure of 1.4MPa (200 psi) can be used. The data were generally obtained from crushing on vertically sided structures, although the ice sheet will likely fail in flexure at the island boundary at pressures less than the crushing pressure. The value of 1.4 MPa is above the envelope containing the highest recorded ice pressure and thus represents a conservative ice strength value.

The above values are consistent with the approach provided in API (1995) and reproduced in Figure 7.3. In this case the design load is based on a constant ice pressure of mean plus 2 standard deviations using data form a number of large-scale measurements. There is not a large amount of data for areas larger than about $10m^2$, and so a constant value of 1.5MPa is advised in that document.

An alternative approach is provided in CSA (2004) for calculating ice pressure. This specification is based on full-scale data from structures such as the Molikpaq in the Beaufort Sea. The ice pressure is given as a function of both ice thickness and aspect ratio. For $80<W/h_i<1000$, the ice pressure can be calculated as presented in Equation 7.5.

$$p_{eff} = C_p h^{D_p} (W / hi)^{E_p} \qquad \text{(Eqn. 7.5)}$$

where h_i is the nominal ice thickness, W is the nominal contact width, and Cp, Dp, and Ep are empirical constants obtained from load measurements. Equation 7.5 is valid for use with SI units, as are the values provided in Table 7.1 which lists the empirical constants based on aspect ratio. Figure 7.4 presents the results of Equation 7.5 graphically for ice thicknesses between 1 and 2m, and structure widths between 50 and 400m, which covers the general range of conditions experienced for ice islands in the Beaufort Sea.

Figure 7.5 presents the range of calculated loads using guidelines given in API (2005), CSA (2004) and using a constant pressure of 1.4MPa as derived from Masterson and Spencer (2000). The CSA (2004) data is presented for structure widths of 100 to 400m. This plot demonstrates the large influence of crushing pressure on the design load.

This approach allows for a substantial reduction in global design pressure when compared with Masterson & Spencer (2000) and API (1995). The values provided in

CSA (2004) assume non-simultaneous failure in a continuously active ice environment and should be allowable for ice island design in landfast ice conditions. This code has not yet been tested in practice, however.

Table 7.1: Constant Ice Pressure Coefficients for High Aspect ratios ($W/h_i > 10$) (CSA, 2004)

Aspect Ratio	C_p	D_p	E_p
$10 \leq W/h_i < 80$	1.5	-0.174	0
$80 \leq W/h_i < 1000$	24.8	-0.174	-0.64
$1000 \leq W/h_i$	0.30	-0.174	0

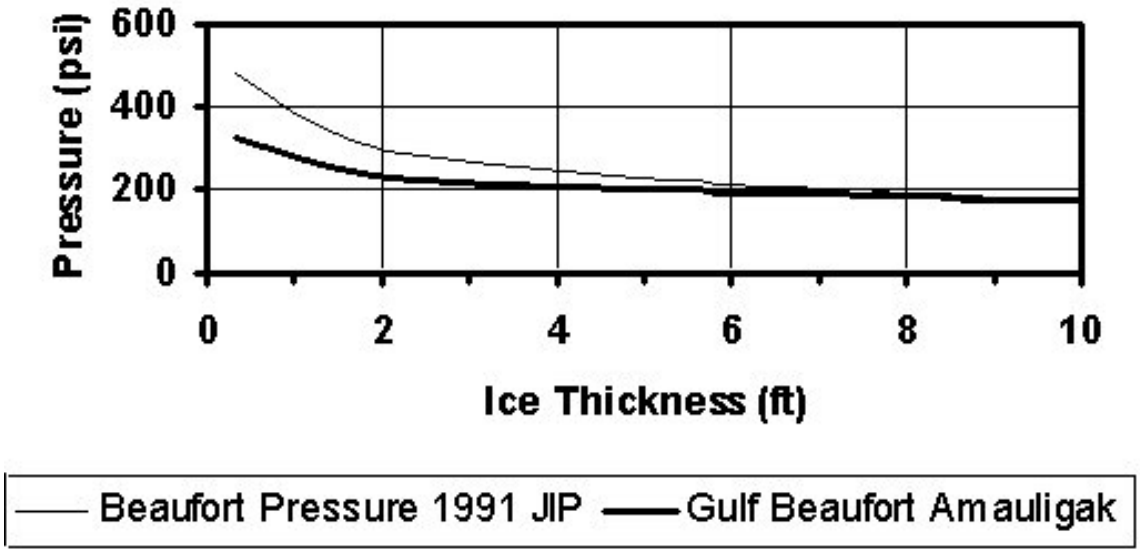

Figure 7.2: Global Ice Crushing as a Function of Ice Thickness (Sandwell 2003b)

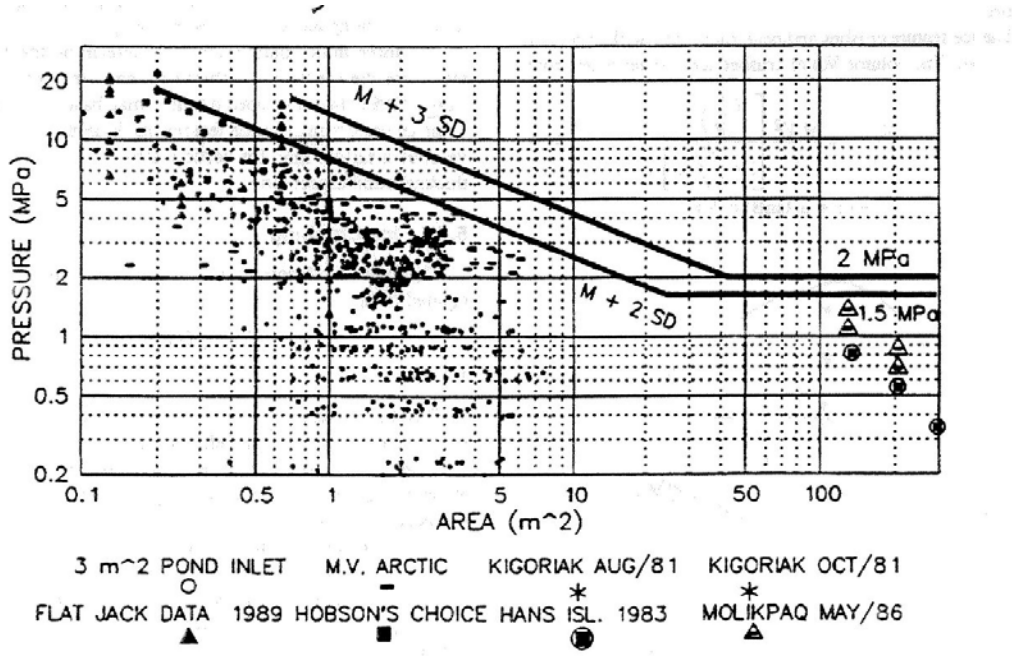

Figure 7.3: Ice Pressure Plot as a Function of Contact Area (API 1995)

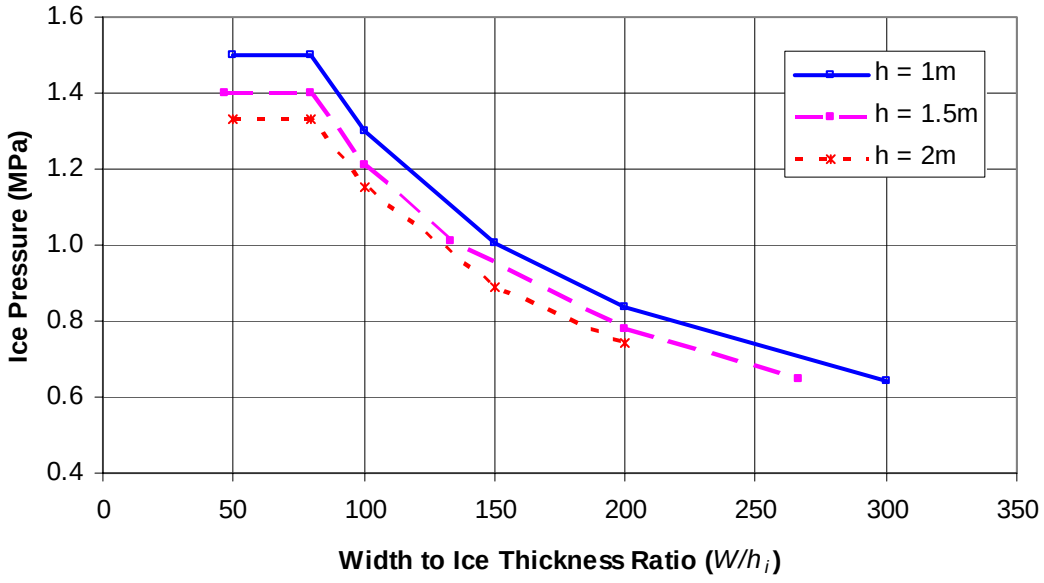

Figure 7.4: Ice Crushing Failure Load Per Unit Width for a Wide Structure (>100m) using CSA (2004) Guidelines

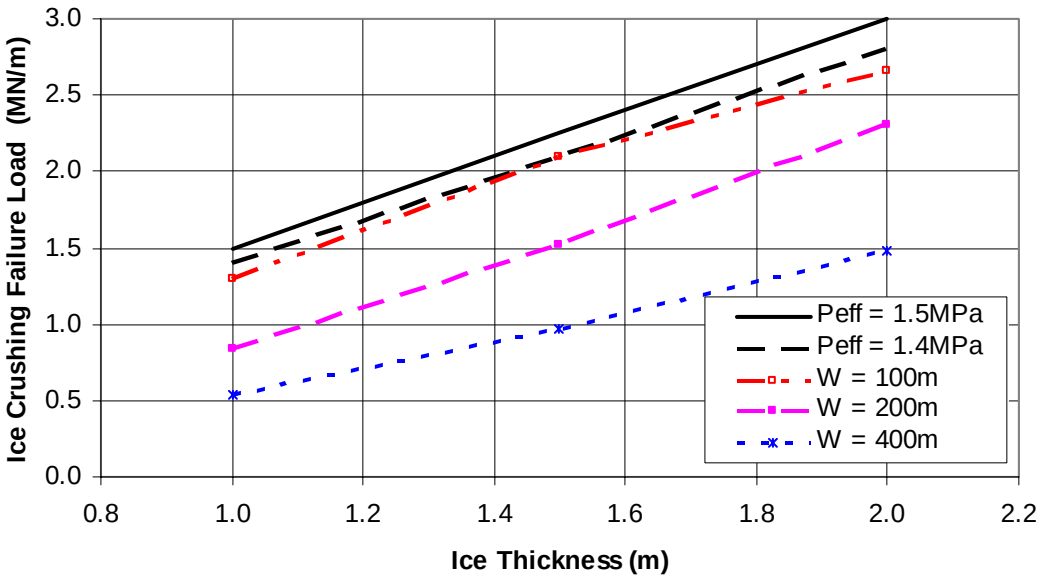

Figure 7.5: Comparison of Ice Crushing Load using Different Guidelines

7.2.3 Passive Edge Failure

Passive edge failure occurs when ice moving in a normal direction to the island fails the leading edge in shear, creating a passive wedge in either an upward or downward direction. Once passive failure occurs, a nominal vertical force due to eccentricities will fail the advancing ice in flexure resulting in a lower ice load than pure crushing. Two methods have been documented in calculating the failure load.

The first method solves for the minimum required island freeboard (height above water level) that will prevent a passive wedge from forming. Weaver and Gregor (1988) used limiting equilibrium theory for a cohesive soil in the analysis of the Angasak spray ice exploration pad. A similar method was also used in the design of the Nipterk Island (Weaver et al 1988). It states that the edge resistance per unit width can be written as (symbols modified for consistency):

$$F_e = \frac{\rho i g H^2}{2} + 2\tau H \qquad \text{(Equ 7.6)}$$

where F_e is the failure load, ρ_i is the above water density of spray ice, g is gravity (9.81m/s^2), H is the height of the island above sea level (freeboard), and τ is the shear strength of spray ice. Note that units should be checked for consistency in Equation 7.6.

It is evident from this expression that failure load is dependant only on the freeboard height of the island and not the thickness of the level ice sheet. If H = 6 m is assumed and using values of τ = 280 kPa and ρ = 640 kg/m^3 (Sandwell, 2003b), F_e = 3.5 MN/m.

The variation in edge failure load, F_e, as it relates to island freeboard is shown in Figure 7.6.

An alternate method of passive edge failure, which allows for a sacrificial failure of the leading edge of the island, has been used in the designs of the Mars Spray Ice Island (Amoco 1985), Karluk Ice Island (Geotech 1988), and most recently the Thetis Ice Islands (Sandwell 2003b). The models developed consider passive wedge failure in both the upward and downward direction as shown in Figure 7.7. These models take into consideration the slope geometry of the ice island and level ice thickness as well as spray ice properties when determining passive failure loads.

Close examination of Figure 7.7 shows that the upward failure plane passes through mostly first-year ice and the downward failure plane passes only through first-year ice. Thus the shear strength that should be used for calculating passive failure will not be that of spray ice but will be that of the first-year ice. Nominally, one can take the shear strength as ½ of the effective ice pressure, p_{eff}.

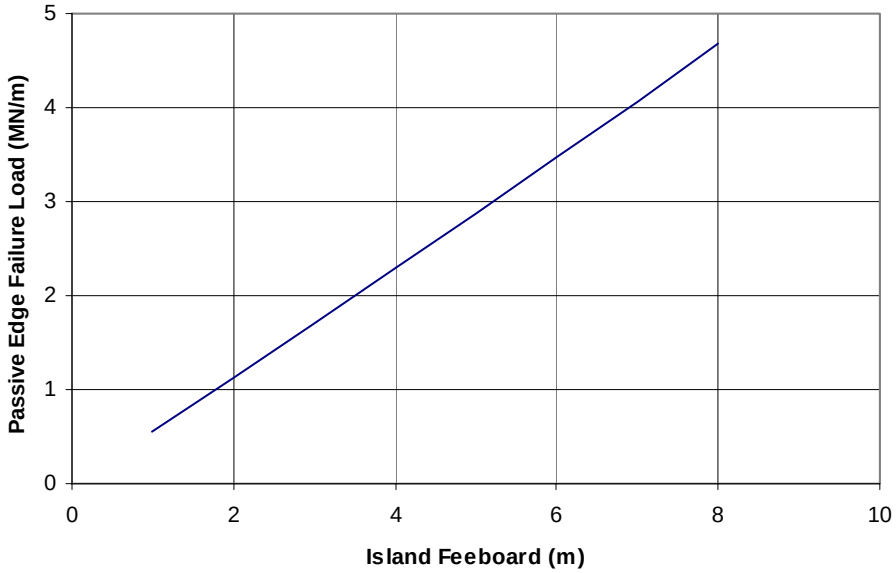

Figure 7.6: Passive Edge Failure Load as a Function of Island Freeboard

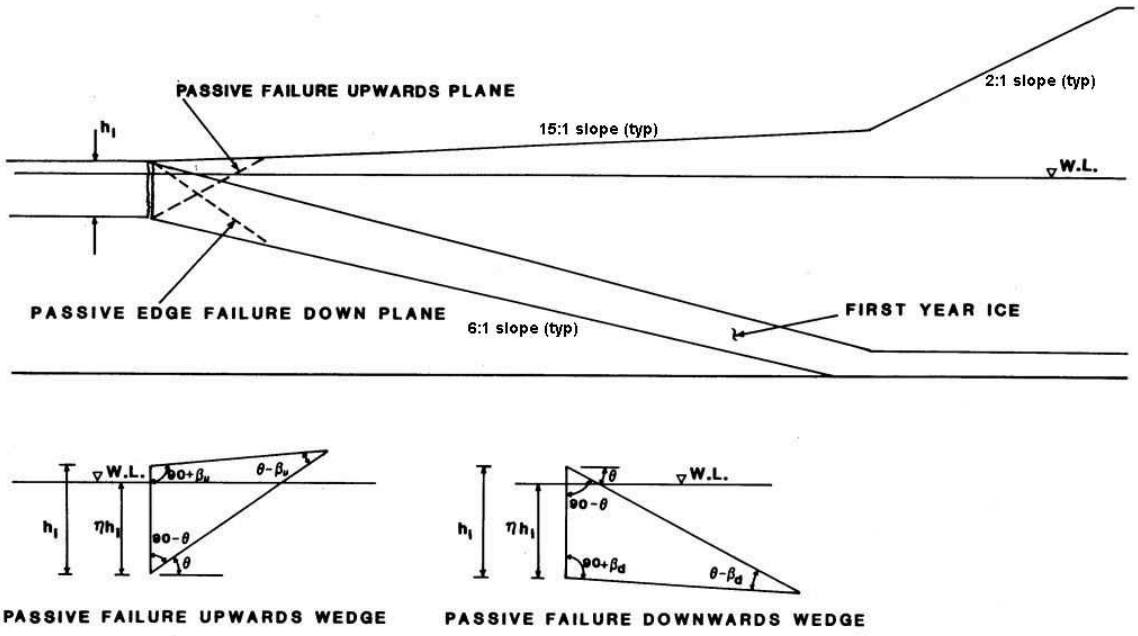

Figure 7.7: Interaction Fringe Passive Failure Scenarios (Geotech 1988)

Consider first, the model for passive upwards failure, as illustrated in Figure 7.8. The limiting passive upwards failure load per unit width, F_{eu}, of island can be determined from:

$$F_{eu} = N(\tan\phi\cos\theta + \sin\theta) + C\cos\theta \qquad \text{(Equ. 7.6)}$$

and solving for θ to obtain minimum F_{eu}, where:

$$N = \frac{-(W + C\sin\theta)}{\tan\phi\sin\theta - \cos\theta} \qquad \text{(Equ 7.7)}$$

$$W = \frac{g h_i^2}{2}\left(\rho_{si}\frac{\sin(90+\beta_u)}{\sin(\theta-\beta_u)}\sin(90-\theta) - \rho_w\eta^2\tan(90-\theta)\right) \qquad \text{(Equ 7.8)}$$

$$C = \frac{c h_i \sin(90+\beta_u)}{\sin(\theta-\beta_u)} \qquad \text{(Equ 7.9)}$$

Where, ϕ is the angle of internal friction of ice (degrees), c is the cohesive strength of ice, θ is the passive failure angle, η is the porosity, ρ_{si} is the submerged density of the ice, ρ_w is the density of seawater and β_u is the above water slope of island edge.

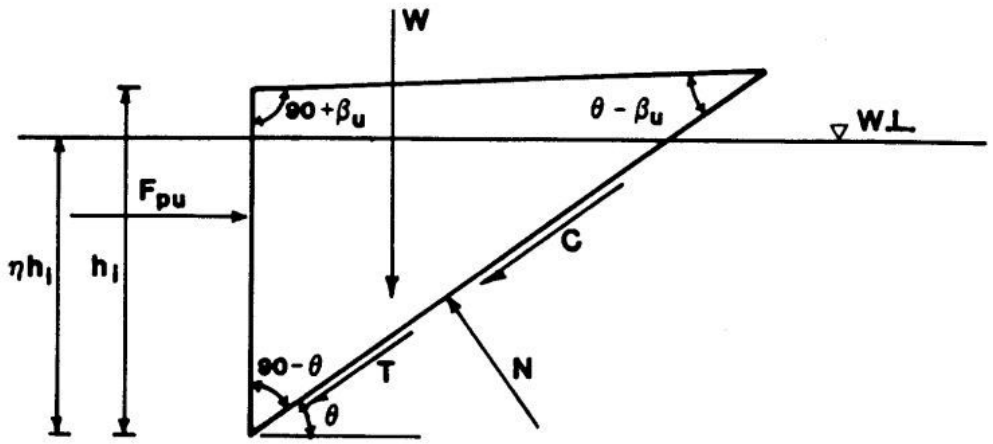

Figure 7.8: Equilibrium Considerations at Incipient Upwards Passive Failure of Interaction Fringe (Geotech 1988)

The edge geometry depicted in Figure 7.7 indicates two distinct upper slopes. The first portion is a shallow slope over the downward deflecting ice sheet followed by a steeper slope over the grounded portion of the island. The upward passive failure is assumed to take place in the shallow sloped upper portion.

Similarly, from Figure 7.9, the limiting passive downwards failure load per unit width, F_{ed}, of island can be determined from:

$$F_{ed} = N(\tan\phi\cos\theta + \sin\theta) + C\cos\theta \qquad \text{(Equ. 7.10)}$$

and solving for θ to obtain minimum F_{ed}, where:

$$N = \frac{W - C\sin\theta}{\tan\phi\sin\theta - \cos\theta} \qquad \text{(Equ. 7.11)}$$

$$W = \frac{g h_i^2}{2}\left((\rho_{si} - \rho_w)\frac{\sin(90+\beta_d)}{\sin(\theta-\beta_d)}\sin(90-\theta) - \rho_w(1-\eta)^2\tan(90-\theta)\right) \qquad \text{(Equ. 7.12)}$$

$$C = \frac{c h_i \sin(90+\beta_d)}{\sin(\theta-\beta_d)} \qquad \text{(Equ. 7.13)}$$

where β_d is the below water slope of island edge.

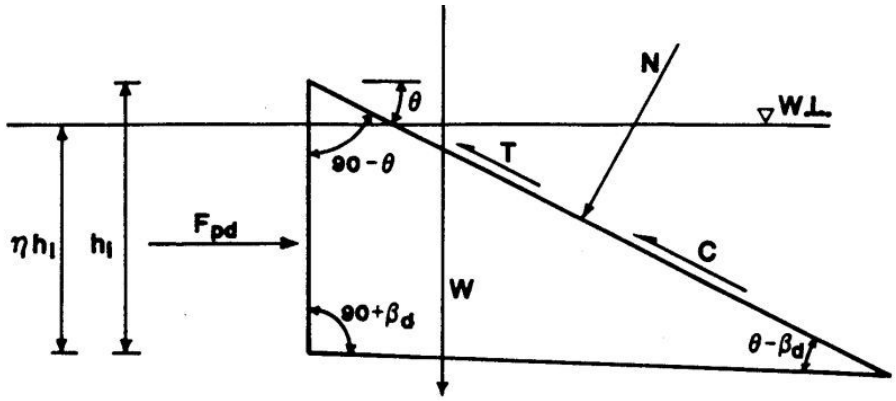

Figure 7.9: Equilibrium Considerations at Incipient Downwards Passive Failure of Interaction Fringe (Geotech 1988)

As an example, the above expressions can be solved for both upward and downward failure by using Thetis ice island geometries and ice properties given as:

β_u = 15:1 slope = 3.81°;
β_d = 6:1 slope = 9.46°;
h_i = 1.7 m;
η = 0.9;
$c = p_{eff}/2$ = 700kPa;
ρ_{si} = 925 kg/m^3 (submerged); and
ρ_w = 1025 kg/m^3.

This provides a solution for upward passive failure load of:

F_{eu} = 2.59 MN/m at θ = 47°.

And downward failure load of:

F_{ed} = 2.86 MN/m at θ = 49°.

The effect of slope angle and ice thickness on F_{eu} is also shown in Figure 7.10 for slope angles ranging from 2:1 to 20:1 and ice thicknesses, h_i, ranging from 1.5 m to 2.1 m. A similar plot for F_{ed} is provided in Figure 7.11.

It should be noted that as the slope angle of the above-water slope increases, the failure plane passes through a greater proportion of spray ice, thereby reducing the average shear resistance of the mechanism. This has not been considered in the above example, which has conservatively neglected this factor. A more rigorous analysis could allow for this, and also for the effect of potentially reduced natural ice thickness at the edge of the island due to construction early in the winter season.

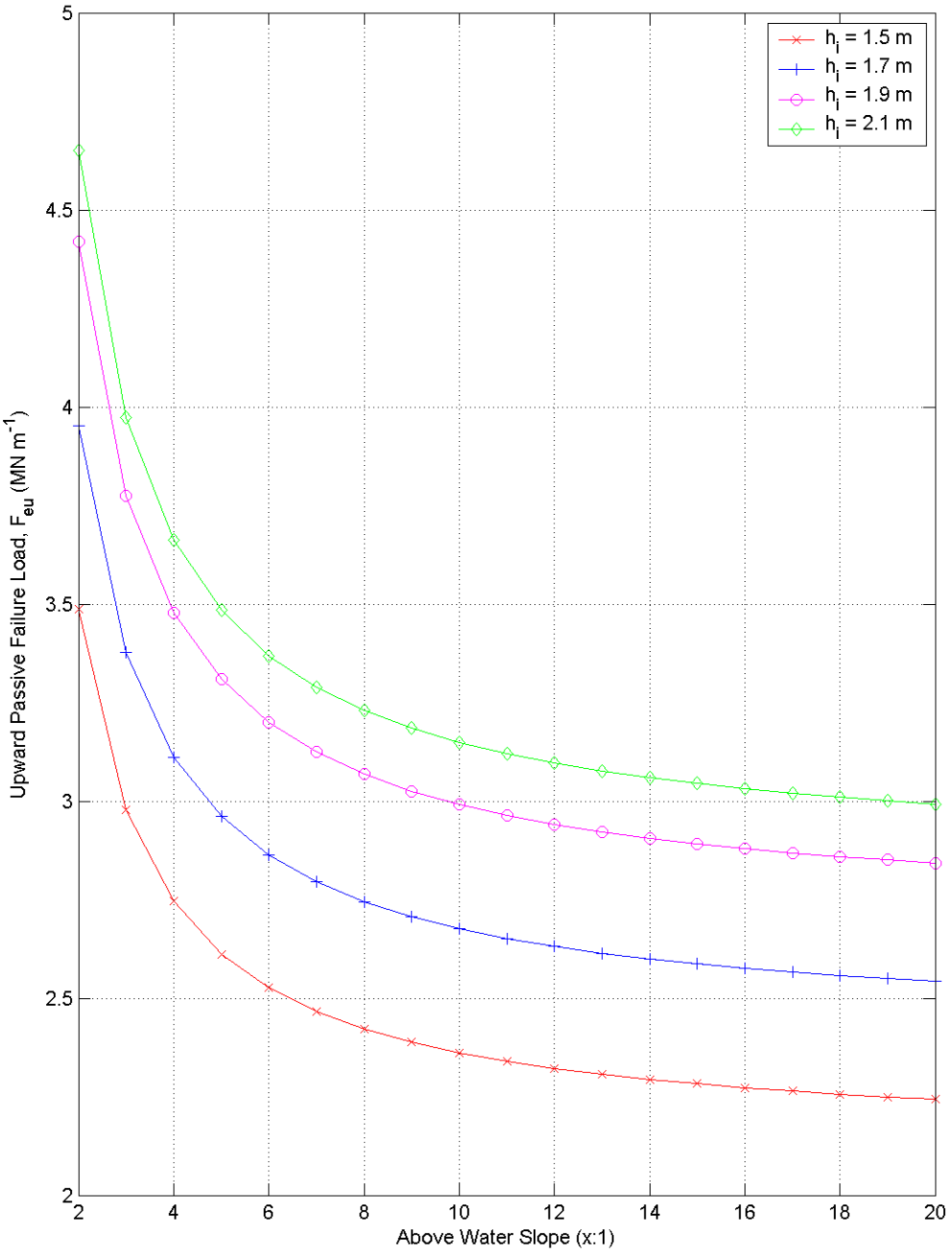

Figure 7.10: Upward Passive Edge Failure Load Based on Above Water Slope and Level Ice Thickness.

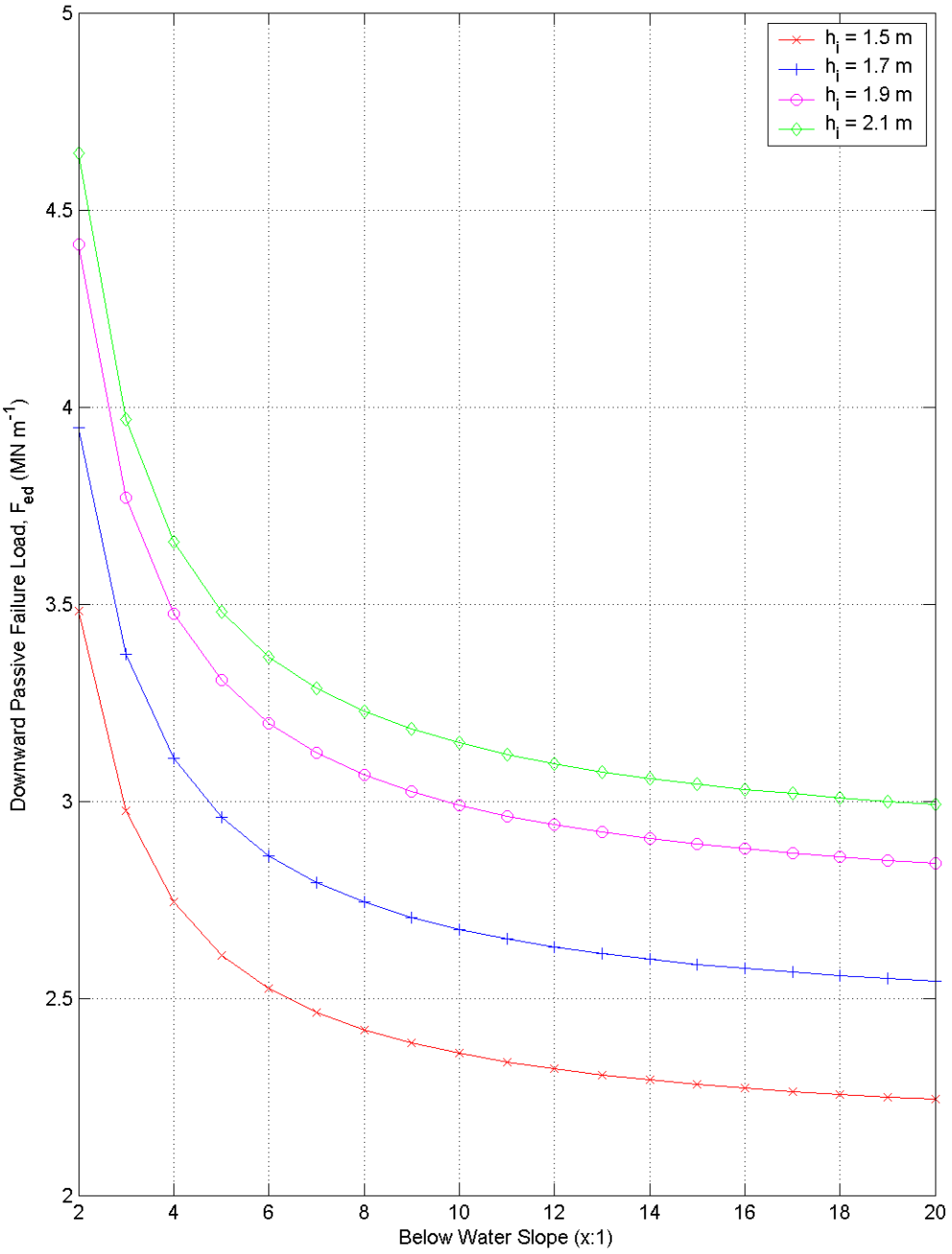

Figure 7.11: Downward Passive Edge Failure Load Based on Below Water Slope and Level Ice Thickness.

7.2.4 Shear failure Within Spray Ice Island

The capacity of a spray ice island to resist shear is determined by the material properties of the spray ice and the plan area of the island core.

$$F_s = \frac{\pi D_c^{\,2} c}{4} \qquad \text{(Equ. 7.14)}$$

where D_c is the island core diameter and c is the cohesive strength of spray ice.

Data presented in Section 6 suggests that in general, the shear capacity of the soil interface below the island is lower than that of the spray ice core and will govern for design.

7.2.5 Sliding Resistance

The ice failure mechanisms can only develop if sufficient sliding resistance is provided between the ice island and the seabed in the form of friction.

The ability of an ice island to resist sliding, due to ice forces is a function of contact area and soil strength, and is determined from the following expression.

$$R_s = \frac{\pi D_c^{\,2}}{4}\left(c_u + (\rho_i g H + (\rho_{si} - \rho_w) g d)\tan\phi_s\right) \qquad \text{(Equ. 7.15)}$$

where R_s is the sliding resistance of the island, D_c is the island core diameter, ρ_i is above water spray ice density, ρ_{si} is below water spray ice density, ρ_w is sea water density, c_u is the bottom material cohesion, ϕ_s is bottom material friction angle, H is island freeboard and d is water depth. A contact factor is sometimes incorporated into Equation 7.15 where soils are predominantly cohesive to account for potential voids between the ice and soil due to uneven grounding. Contact values of 0.85 or 0.9 have been used (Weaver & Poplin 1997).

The above calculated resistance assumes that the shear resistance at the interface between ice and soil is lower than shear through the ice core. This is usually the case for the relatively low strength soils found in the Canadian and Alaskan offshore Arctic.

The seabed soil type has an important effect on the design of the island in providing adequate sliding resistance, and the design approach should reflect differences between soil type.

The strength of a clay soil is defined by the undrained shear strength (cohesion), which is independent of applied confining pressure when acting in an undrained manner. The sliding resistance is therefore governed by the contact area between the grounded island

and the seabed. Enhanced capacity may be attributed to penetration of ice into the clay seabed, particularly in soft soils, whereby the ice extends to higher strength clay. Some passive wedge resistance may also be available depending on the penetration depth. The main aim in determining allowable shear resistance is to ensure adequate contact pressure to develop shear failure at the ice/soil interface. A bearing pressure of about 25kPa is considered acceptable (Weaver & Poplin 1997). Underwater currents are generally low in the shallow-water Arctic, and there are no known reported cases of current scour or erosion being a concern at previous ice island sites.

The seabed in many areas of the arctic offshore consists of very soft clay at mudline, increasing strength with depth. A seabed undrained shear strength of 10kPa is common, although higher values can be utilized where strength increases rapidly with depth. A number of methods have been considered in order to improve sliding resistance, including (St Lawrence 1992):

- Pre-consolidation to increase the shear strength - consolidation of the seabed surficial materials takes place when the island is grounded with sufficient surcharged in the form of large enough freeboard. A freeboard of about 4.5m is therefore usually specified for an island placed on cohesive soils to ensure sufficient seabed contact pressure for both generation of shear resistance and enhanced soil strength.

- Deeper penetration of the ice to reach more competent soils or removal (dredging) of the weak clay layer – Some penetration of the soft surficial soils does take place, although the determination of the degree to which this occurs is difficult to calculate. Dredging activities would significantly increase the cost of the ice island, as mobilization of suitable specialist equipment to the Beaufort Sea would be expensive.

- Penetration of the soft clay with piles to bear on stronger strata - piles are not likely to be practical for ice islands, as they would be ineffective in addressing lateral shear resistance and it would be impossible to install sufficient piles within a single winter season. They would not be required for bearing capacity under the rig loads as the ice has more than ample strength for this purpose, as evidenced by the performance of past islands.

- Freezing of the seabed - this is also considered impractical using current technology as it would have to be done with complex installations performed the year before the island was built and the well drilled. The cost would therefore likely be prohibitive.

The sliding resistance of an ice island grounded on sandy soils is a function of the internal angle of friction of the soil and applied normal (vertical) stress. Increased bearing stress, by increasing the freeboard of the island, will act to increase shear resistance that can be mobilized at the soil/ice interface. Increasing the freeboard allows the contact area to be reduced while maintaining the resistance, and could therefore be

used to develop an optimum economical solution. Limits on the maximum practical freeboard would depend on spray equipment capacity and the time available to build an island. The achievable vertical build-up rate is controlled by the time required to freeze and cure the spray ice as it is applied. Access ramps would also become steeper or longer as a function of increased freeboard, increasing the volume of ice required for these structures.

The sensitivity of the sliding resistance is demonstrated in Figures 7.12 and 7.13 for clay and sand seabeds as a function of freeboard (which determines applied stress). A typical geometry taken from the Thetis Ice Islands (Sandwell 2003b) has been used, along with nominal clay undrained shear strength of 25kPa and sand internal angle of friction of 30^{o}. The figures compare the required available sliding resistance as a function of island diameter, assuming crushing of a 2m thick ice sheet with 1.4MPa applied ice pressure. A water depth of 6m has be4en used. Comparison between the calculated resistance and applied ice load provides the factor of safety. A factor of safety in the range of 1.35 to 1.5 has been used on previous operational islands. The results show the required island diameter to resist ice loads for each of 3m and 6m freeboard, and quantifies the potential benefit of reduced island diameter by considering increased freeboard on a sand seabed.

A reduced island diameter can substantially reduce the required ice volume as demonstrated in Figure 7.14. Since the required working area from a drilling operations point of view is likely to be of the order of 100 to 200m, large savings in construction cost are possible by optimizing the design such that this requirement is not exceeded. The freeboard has no effect on the island diameter required on a cohesive clay seabed, although as discussed above, a minimum freeboard is required to ensure solid contact between the island and the seabed.

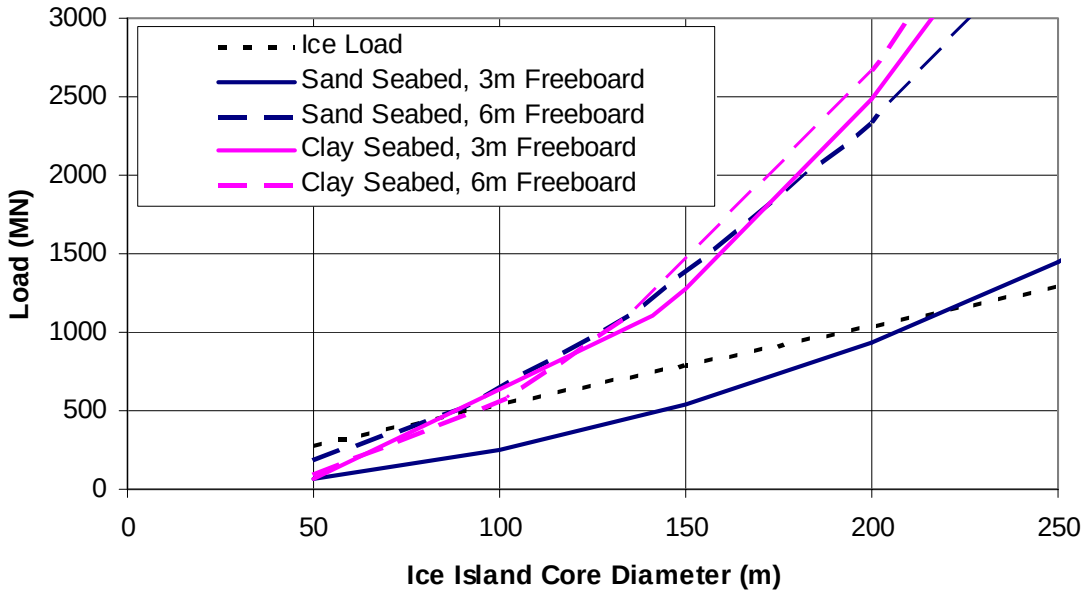

Figure 7.12: Comparison of Allowable Sliding Resistance for Ice Islands Grounded on Clay and Sand Seabed

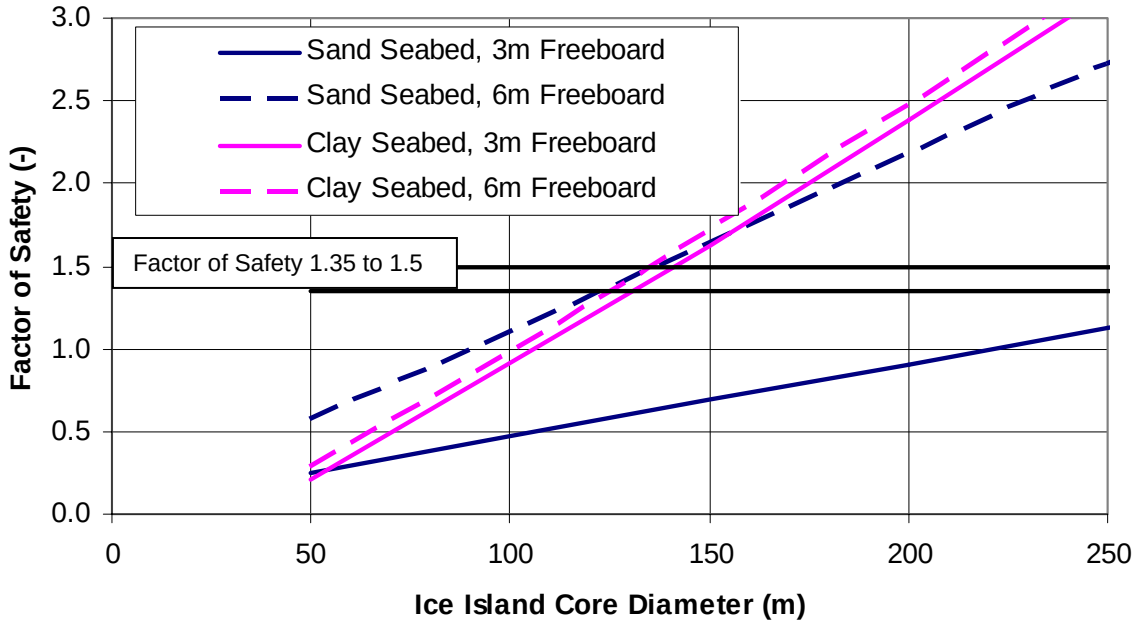

Figure 7.13: Comparison of Factor of Safety Against Sliding for Ice Islands Grounded on Clay and Sand Seabed

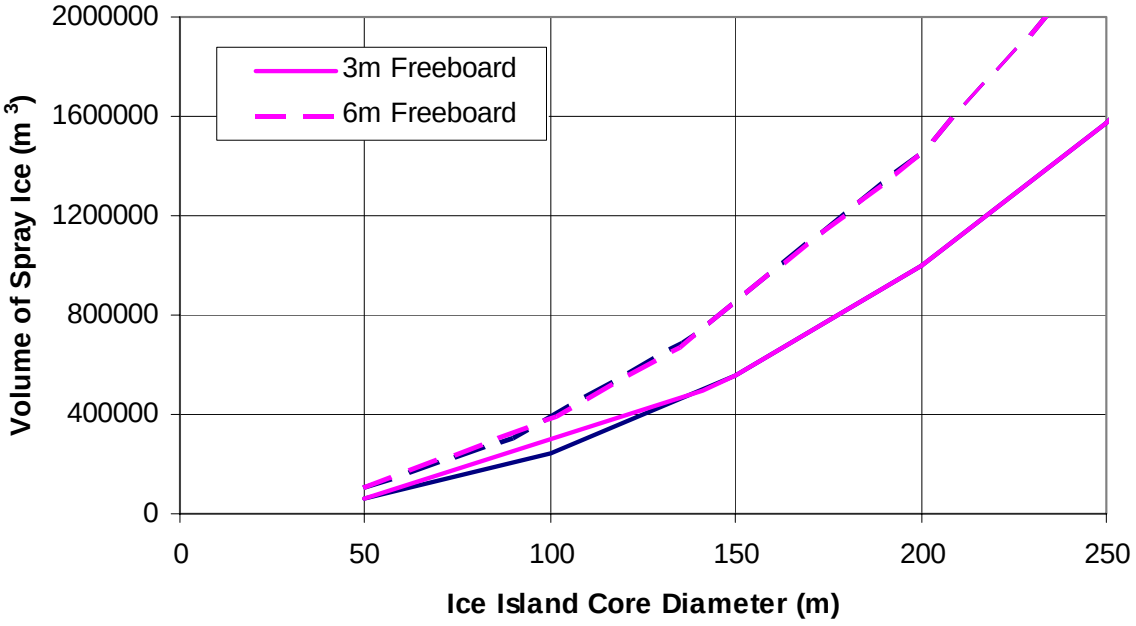

Figure 7.14: Volume of Spray Ice as a Function of Island Diameter and Freeboard

The design analyses described considers the island to act as a rigid body subject to uniform load and stress conditions. This simplified model is convenient and has been shown to provide an acceptable level of confidence in design. However, it should be recognised that the island is not rigid, but acts as a continuum in which compression and distortion occurs. Figure 7.15 presents an idealized combined deformation and sliding movement model.

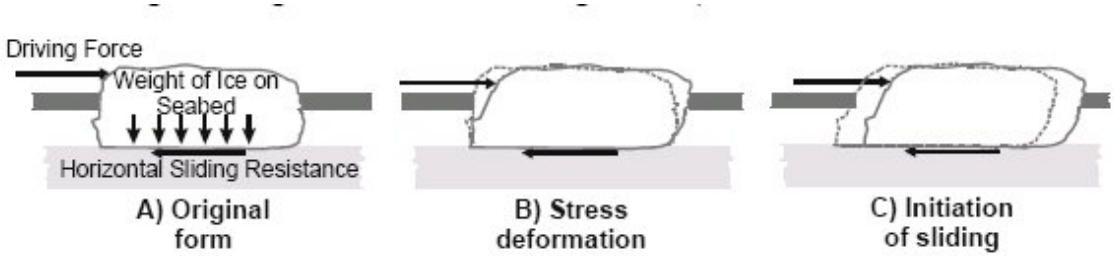

Figure 7.15: Schematic of Combined Deformation and Sliding Mechanism (Barker & Timco 2004)

Nipterk Island (Weaver & Poplin, 1997) was closely monitored during ice loading events, and differential horizontal movement of the island was correlated with a simple soil shear model to assess ultimate resistance. Important points to note were that island compression was measured at greater than 200mm probably partly due to the presence of cracks in the island core. It is therefore conceivable that significant movement at the conductor location could be experienced before reaching the island sliding resistance, and this servicibility limit state should be considered in design. More rigorous modeling of ice islands under load would allow more representative design assumptions to be made. Figure 7.16 shows the sliding movement at the seabed for Nipterk Island, interpreted from inclinometer readings. This demonstrates that significant movement of the island core can occur before full mobilization of shear resistance.

On the other hand, ice interaction with the island, would be expected to result in more deformation at the edges than at the centre. The deformation across the island is not uniform and is concentrated at the leading edges where the force is applied. Deformations thus seen at the edge are likely to be significantly less at the conductor location, which is usually located in the central part of the island. Thus more exact analysis would determine the importance of movements occurring near the edge due to ice movement.

Current design methodologies consider sliding along a flat interface between the ice and seabed soil at mudline. In reality, the natural ice sheet breaks up as it is loaded and depressed during construction, and is likely to penetrate into the seabed in a non-uniform manner, with voids becoming filled with displaced soil. This would be particularly evident with soft clay soils. Skirting action due to penetration, mobilization of stronger soil at the depth of penetration and potential consolidation of soft clay soils may all contribute to higher shear strength under sliding. Some of these considerations were investigated in the demonstration centrifuge test with the aim of identifying any dominant mechanism that may allow improved design methodologies. The results of the centrifuge test are reported in Section 12.

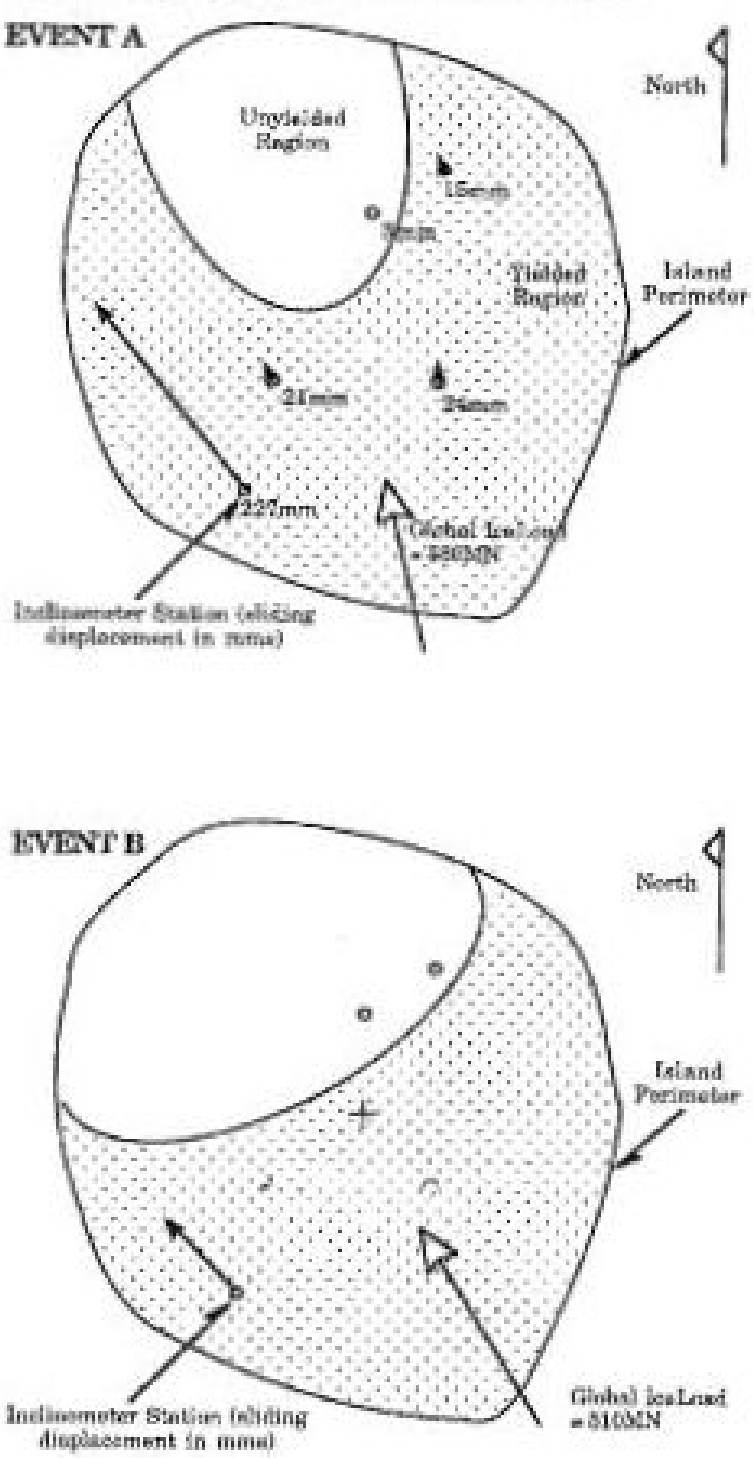

Figure 7.16: Ice Island Seabed Movement at Nipterk (Weaver & Poplin 1997)

7.2.6 Example Ice Load Analysis

The following is an example to illustrate the application of the design process described in the preceding sections and how selection of design failure mode influences the final dimensions of the island. Assumed values include: water depth of 6 m and a maximum expected level ice thickness of 2 m. A sand seabed with angle of internal friction, ϕ_s=30^o was used. Ice island edge geometry and spray ice properties were based on typical values at the Thetis site, presented in (Sandwell 2003b) and given in Section 7.2.3. A factor of safety of 1.3 was used.

Other factors influencing island dimensions, such as minimum required footprint for equipment placement, spray ice creep settlement and other possible requirements, were not considered.

Base Case: Level Ice Crushing Load (Rigid Body Sliding):

$$R_s = 1.3\ F_c W \qquad \text{(Equ. 7.16)}$$

where: F_c = 2.8 MN/m (for 1.4MPa ice pressure, 2m thickness)

W = effective width of island

$$= D_c + 2\ \mathrm{H}\ \beta_u \qquad \text{(Equ. 7.17)}$$

where:

β_u = slope of upper island taper closest to core (2:1)

= 2

Substituting Equ. 7.15 and Equ. 7.17 into Equ. 7.16 achieves a solution for core diameter, D_c, with respect to freeboard height, H. The summary of results is presented below in Table 7.2. Core diameter against freeboard is also shown in Figure 7.15.

Table 7.2: Ice Island Dimensions to Satisfy Base Case Load Scenario – Level Ice Crushing

Core Diameter (m)	**Island Freeboard (m)**	**Effective Width (m)**	**Sliding Resistance (MN)**
640	3	652	2340
428	4	444	1590
322	5	342	1230
258	6	282	1010
216	7	244	875

Passive Edge Failure, Flexural Ice Failure:

If the outer edge of the island is deemed to be sacrificial, the initiation of flexural ice failure due to passive edge failure can be considered using Equ. 7.6 and Equ. 7.10 outlined in Section 7.2.3.

Given the shallow upper slope of 15:1, a bottom slope of 6:1 and 2 m ice thickness, we can solve for both above and below water passive failure loads.

F_{eu} = 2.59 MN/m
F_{ed} = 2.86 MN/m

Since F_{eu} governs, we can now solve for sliding resistance.

$$R_s = 1.3\, F_{eu} W_{eff} \qquad \text{(Equ. 7.18)}$$

This provides a solution for core diameter, D_c, with respect to freeboard height, H. The summary of results is presented below in Table 7.3. Core diameter against freeboard is also shown in Figure 7.17.

Table 7.3: Ice Island Dimensions to Satisfy Passive Edge Failure Scenario

Core Diameter (m)	**Island Freeboard (m)**	**Effective Width (m)**	**Sliding Resistance (MN)**
599	3	611	2059
401	4	417	1405
302	5	322	1084
242	6	266	896
202	7	230	775

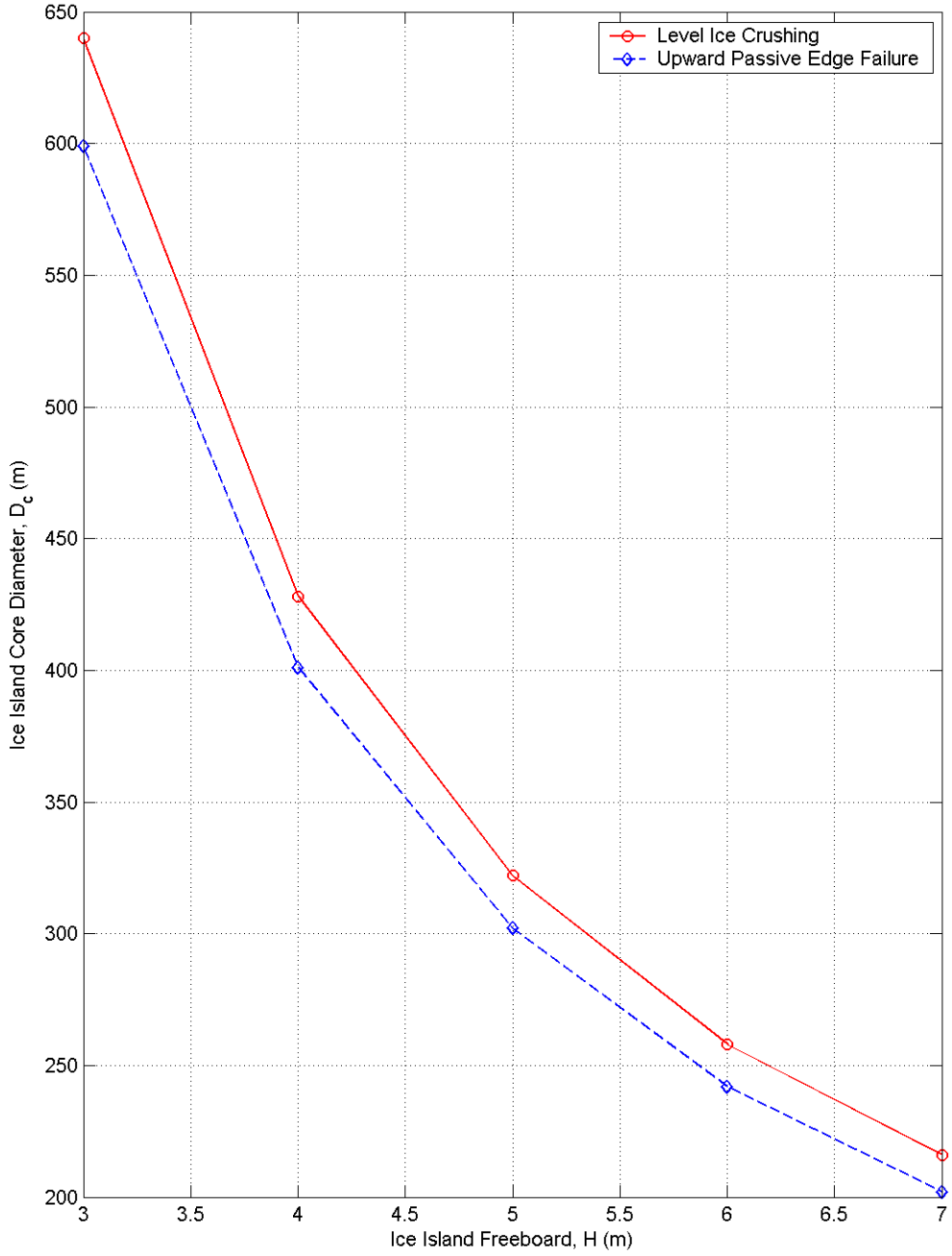

Figure 7.17: Requirements for Ice Island Freeboard, H, and Core Diameter, Dc, Based on Ice Load Resistance Criteria.

The design example has been repeated for the lower ice pressures calculated using the CSA (2004) approach as discussed in Section 7.4. Solutions for core diameter, D_c, with respect to freeboard height, H, for the level ice crushing model are shown in Table 7.4. All other values were the same as for the original design example.

Table 7.4: Ice Island Dimensions to Satisfy Ice Crushing Based on CSA (2004).

Core Diameter (m)	Island Freeboard (m)	Effective Width (m)	Sliding Resistance (MN)
360	3	372	768
280	4	296	704
240	5	260	700
200	6	224	626
180	7	208	626

Similarly, solutions for core diameter, D_c, with respect to freeboard height, H, for passive edge failure using a value for level ice shear strength equal to one half of the effective pressure are shown in Table 7.5.

Table 7.5: Ice Island Dimensions to Satisfy Passive Edge Failure, Based on CSA (2004).

Core Diameter (m)	Island Freeboard (m)	Effective Width (m)	Sliding Resistance (MN)
380	3	392	852
290	4	306	753
250	5	270	757
210	6	234	686
190	7	218	692

The results from Tables 7.4 and 7.5 are also shown in Figure 7.18. The results from the original design solutions are also shown for comparison.

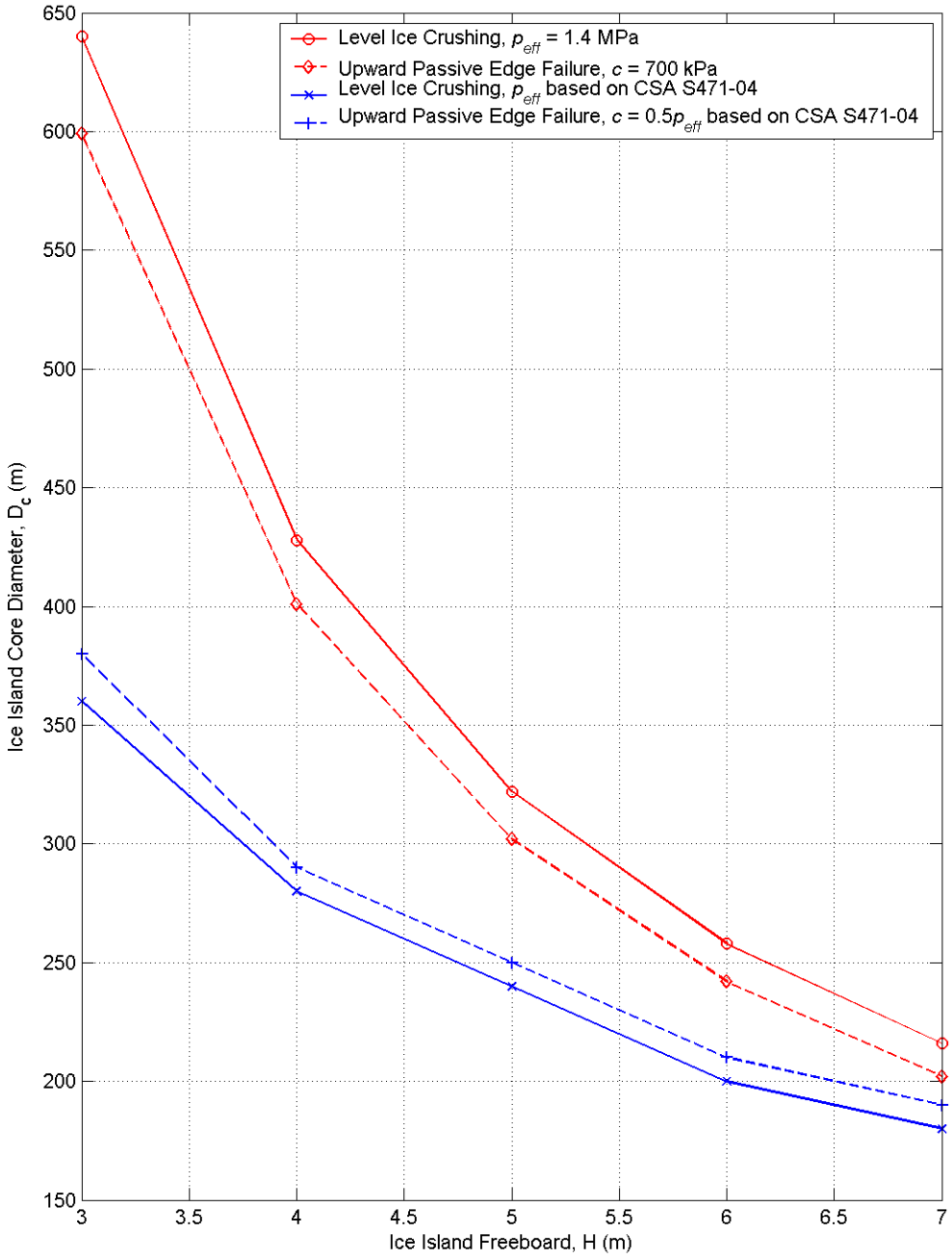

Figure 7.18: Comparison of Island Diameter vs. Freeboard based on Ice Load Resistance Criteria

The sample design load calculations above indicate little difference in the required ice island dimensions based on selection of failure mode (level ice crushing or passive edge failure). In fact, using ice pressures recommended in CSA (2004), level ice crushing failure results in a slightly lower load than passive edge failure. In both cases, the difference is generally less than 5%.

The more significant difference, however, results from the assumptions made in establishing the global ice pressure. The CSA (2004) method provides significantly lower forces, which allows the resulting island to be built using less material. Table 7.6 provides a comparison of the volume that would be required to achieve the design criteria using each method, showing the potential savings that would result.

Table 7.6: Comparison of Ice Crushing Design Criteria using Constant Ice Pressure and CSA S471-04

Island Freeboard (m)	Constant Ice Pressure		CSA S471-04		Reduction in: (%)	
	Core Diameter (m)	Total Spray Ice Volume (m3)	Core Diameter (m)	Total Spray Ice Volume (m3)	Core Diameter	Total Spray Ice Volume
3	640	2596776	360	812371	44	69
4	428	1320037	280	564654	35	57
5	322	847996	240	474751	25	44
6	258	617414	200	376954	22	39
7	216	490514	180	347048	17	29

A number of practical issues and uncertainties must be addressed in the design of the sliding resistance of an ice island as discussed above. Barker and Timco (2004) identified and listed these factors to be considered as part of the design. Table 7.7 summarises these concerns as follows:

Table 7.7: Summary of Issues for Ice Island Design

Vertical Load	**Horizontal Load**	**Friction and Cohesion / Adhesion**
Height of ice pad	Environmental driving force	Local / global failure of rubble
Diameter of ice pad	Ice sheet thickness	Seabed cohesion
Waterline location	Ice velocity	Seabed friction angle
Porosity of spray ice	Failure mode at the edge of pad	Nature of the ice / seabed interface
Compressibility of ice rubble	Ice rubble cohesion	
Drainage channels	Ice rubble friction angle	

8.0 ICE ISLAND CONSTRUCTION

As discussed in Section 5, construction techniques evolved through the 1970s and 1980s as greater efficiency and reduced construction time was required to meet operational constraints. The use of flooded ice construction has largely been superceded with spray methods for cases where large volumes of ice are required, such as offshore exploration platforms. This section will focus on the use of spray ice technology for construction of grounded islands, although other techniques are advantageous under certain conditions eg. final leveling of ice roads.

8.1 Construction Season

The scheduling of a winter offshore drilling program using an ice island in Arctic regions using current techniques is governed by the following environmental conditions:

- Sufficient build-up of landfast ice thickness to support construction equipment to start ice island construction;
- Sufficient ice road load capacity to support rig demobilization on completion of drilling;
- Weather conditions during the winter construction season, such as wind and temperature.

An additional requirement to which drilling programs have been subject was to allow time to drill a relief well in the event of a blow-out of the main well. This would usually require prior construction of a separate drilling platform and access road, standby of a rig and time to undertake a relief well between the end of scheduled drilling and last demobilization date. This may be the critical factor in establishing latest well completion time.

Generally, freeze-up in the Beaufort Sea starts in mid October and ice increases in thickness at an average rate of about 1cm per day as shown in Figure 8.1. Formation of landfast ice extends to water depths of 10m in Harrison Bay by early December and 20m by early January (ORourke 1984). Data from the Canadian Beaufort suggests a slight lag, with landfast ice reaching the 10m contour by mid-December and 15m by end of January (Poplin 1990). An ice thickness of approximately 80cm is deemed sufficient to start construction using light equipment for road construction with a view to increasing thickness sufficiently to start island construction using large pumps in December.

The time required for construction of a spray ice island is a function of the required volume, environmental conditions (temperature, wind etc.), equipment used and construction methodology adopted. Table 8.1 presents data on the start and completion time for a number of spray ice structures in the arctic. A review of operational islands (marked by * in Table 8.1) used for exploration in the Arctic shows that construction time

has taken between 20 and 60 days, with the average being 30 days. Details of specific issues related to equipment used and spray efficiency are discussed in following sections.

The duration of a drilling program in the Arctic depends on a number of factors, which are beyond the scope of this report. Data for offshore wells drilled in the Beaufort Sea suggests that a period of 30 to 45 days should be allowed to complete a well and demobilize a rig. Closure of ice roads generally start in late April to late June, depending on the area, with consideration given not only to the offshore grounded or floating offshore road, but also to the requirement to transport the rig back to some staging area onland. While transportation infrastructure on the Alaskan North Slope is in place, the closure of ice roads in the Canadian Mackenzie Delta leave the region largely inaccessible by road during the summer months. The Mackenzie Delta area is, however, accessible by river and sea during the summer months.

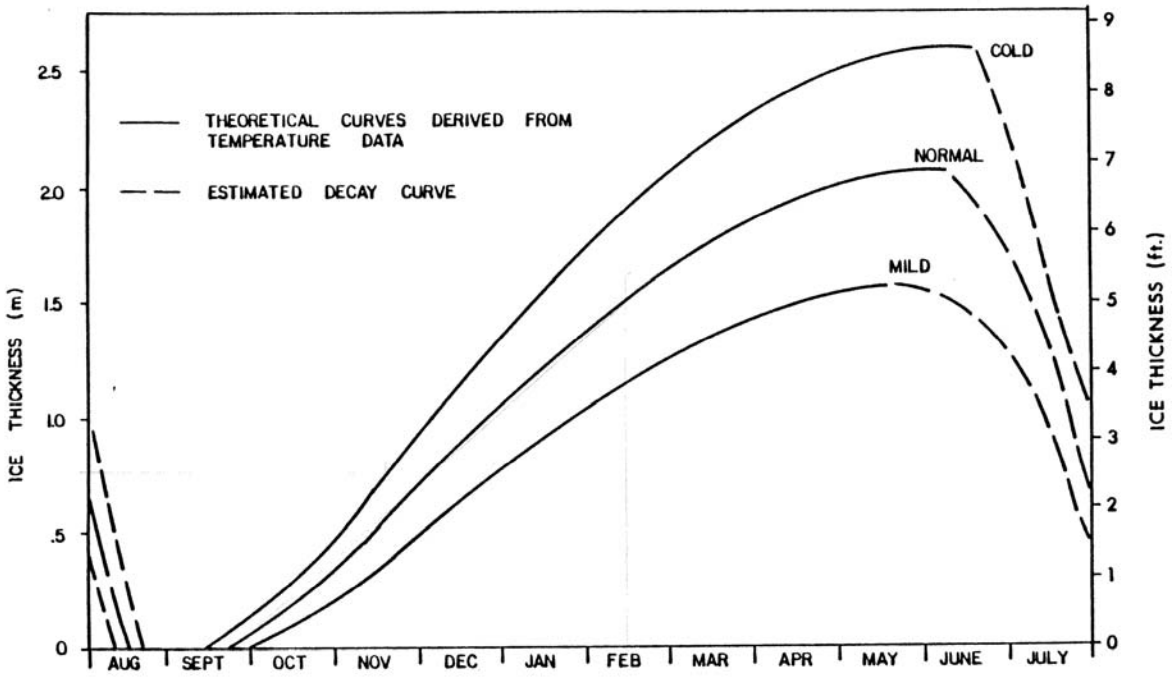

Figure 8.1: Typical Ice Thickness Growth Curve for Canadian Beaufort Sea

Table 8.1: Construction Time for Spray Ice Structures

Structure	start date	end date	Construction Time (days)
Tarsiut Relief Ice Pad	late Nov.	Jan.	70
Alerk island	27-Jan-82	10-Feb-82	14
SSDC Uviluk	20-Dec-82	20-Mar-83	41
Sohio Rubble Generator	3-Dec-83	17/01/84	45
Exxon Ice Island Experiment	29-Dec-83	19-Jan-84	21
Big Gun Expt	31-Dec-83	19-Jan-84	20
SSDC Kogyuk	2-Nov-83	23-Jan-84	73
CIDS Antares Barrier	22-Oct-03	21-Dec-03	60
Kadluk 0-07		12-Dec-83	35
Cape Alison C-47	3-Dec-84	16-Jan-85	44
MARS full-scale prototype	1-Feb-84	1-Mar-84	30
Mars*	8-Jan-86	23-Feb-86	45
Angasak L-03*	7-Dec-86	3-Feb-87	58
Nipterk P-32*	28-Nov-88	20-Jan-89	53
Karluk*	13-Dec-88	20-Jan-89	38
Ivik*	24-Jan-03	17-Feb-03	24
Oooguruk*	24-Jan-03	7-Mar-03	42
Natchiq*	11-Feb-03	4-Mar-03	21
Kashagan, Sunkar Site	13-Dec-02	2-Jan-03	1.5
Kashagan, Aktote Site			
Kashagan, Kairan Site			

8.2 Spray Ice Equipment

A range of spray equipment has been used during both trials and operations to establish the most efficient manner of island construction. Since the construction schedule is critical to the success of a drilling program, the aim is to produce the required volume of ice at the greatest rate possible. Various techniques have been developed to improve the production rate of ice, including continuous spraying and spray/cure cycles that allow a cold ice temperature to be maintained throughout the island. Procedures have also been developed to account for changes in temperature and wind speed, in order to maintain optimum ice production.

Two main types of pump have been used to date – large units mounted on floating or fixed structures such as the Kigoriak and CIDS, and smaller skid mounted pumps supported directly on the landfast ice. The weight of skid mounted pumps is restricted due to difficulties of transportation to the work site, ice thickness requirements and difficulty of moving around the ice platform to deal with changing wind conditions and build-up geometry. Vertical turbine and horizontal centrifugal pumps have been used for spray ice formation in the arctic offshore. Vertical turbine (submersible) pumps have the pump located underwater and are not susceptible to freezing of the suction lines, as drainage of the lines is immediate as soon as the unit is stopped. However, centrifugal pumps provide an advantage when pumps need to be moveable across the ice on skids, in that the pump is not submerged below the ice surface, which would require that the drive

shaft to be disconnected from the engine and the pump raised before an move is possible. Alternatively, it is a relatively simple matter to remove an insulated intake pipe from a centrifugal pump.

Design of the nozzle and monitor is important in determining the spray configuration as it exits. The most commonly used system is a standard hollow cone used in fire fighting, that can be adjusted from straight stream to a fine mist. The production of a fine mist produces small diameter water droplets which freeze in an efficient manner, but are also more susceptible to being carried away from the target by winds. A straight jet, which provides the greatest horizontal throw range is therefore widely used and allows the jet to remain in contact with the air for the longest period. Depending on wind conditions, an angle of 45^o to 60^o is considered optimum for maximum ice production.

Experiments have been carried out to establish the effect of pump volume flow and nozzle pressure capacity on production rates. The effect of temperature on production of spray ice has been discussed in Section 6.3. Measurements have been made to establish the efficiency of production, based on both ice produced from a given volume of pumped water, and also percentage of ice landing in the target area. The second parameter is particularly sensitive to water droplet size and wind speed, as well as target size and flexibility of pump positioning. Table 8.2 presents data from a range of sources on the capacity of various pumps and nozzles configurations. Table 8.3 presents data on the calculated efficiency of pumps, where the volume of spray ice landing on target was measured as a ratio of pumped water. Further discussion of the various spraying equipment is provided in the following paragraphs.

A review of equipment for forming spray ice was performed by Allyn and Masterson (1989). A pump pressure of the order of 1400kPa is considered a minimum requirement to achieve adequate throw distance and to ensure atomization of the water stream as it exits the nozzle. Experience with lower pressure pumps of 300 to 400kPa has proven unsatisfactory. An exit velocity from the nozzle of 50m/s is stated as desirable to ensure the required spray behaviour.

Practical experience suggests that two to four large pumps, with a minimum volume flow rate of the order of $10m^3$/min (167 l/sec) are required to efficiently produce the ice required to construct a typical grounded ice island. The requirement to position the pumps near the circumference of the island to allow access to water, whilst providing the required throw distance to cover the island area suggests that smaller pumps would not be suitable due to the number of pumps that would be required to produce the volume of an island.

The use of additives to enhance ice production, particularly at warm temperatures has been met with limited success (Masterson et al, 1987), although higher concentrations may have produced better results. The potential benefit of a bacterial additive "Snowmax" was reported by Collins & Masterson (1989), although no evidence of its use in practical situations for the construction of ice islands was found. The incorporation of

compressed air to reduce droplet size, and nucleation particles to aid the freezing process have a sound theoretical basis, but have not been found to provide enough of an advantage to be used routinely in the field. A practical limitation of air injection is that the volume of air required would be large and would require an air compressor larger than the water pump, thus greatly complication logistics. Freezing of the air intake on the compressor would be a constant problem, which would require the use of filters and pre-heaters.

APPLICATION	LENA RIVER CROSSING	ALERK ISLAND	SSDC UVILUK		ESSO BIG GUN EXPERIMENT	SOHIO RUBBLE GENERATOR	SSDC KOGYUK			
SPONSOR	USSR	ESSO RESOURCES LIMITED	CANMAR LIMITED		ESSO RESOURCES LIMITED	SOHIO	CANMAR LIMITED			
SITE DETAILS										
TOTAL AREA m^2	N. A.	5500	25 000		NOT FIXED	20 000	29 000			
TOTAL WEIGHT TONNES	N. A.		200 000				183 000			
SPRAY SYSTEM										
NAME	NSP 75/100	AURORA	SSDC BALLAST	TAIT 15 HP	THUNE EUREKA EF 400	TAIT 100 HP	THUNE EUREKA EF 400	SSDC BALLAST	KIGORIAK FIRE PUMP	TAIT 15 HP	THUNE EUREKA EF 400
NUMBER OF OUTLETS	1	1	12	6	1	2	1	13	1	6	1
NOM. POWER/OUTLET kW	92	78	(15)	11	1627	75	1627	(15)	28	11	1627
NOM. FLOW RATE ℓ/sec.	75	75	42	35	1000	32	1000	42	42	35	1000
NOM. PRESSURE kPa	981	827	289	240	1310	1448	1310	289	520	240	1310
START DATE	1980	82-01-27		82-12-20	83-12-31	83-12-03	84-01-19	83-11-02	83-11-05	83-11-26	84-01-26
FINISH DATE	1980	82-02-10		83-03-20	84-01-19	84-01-17	84-01-24	84-01-23	83-11-13	84-01-24	84-02-01
NOZZLE DIAMETER mm	35 | 45 | 55	38	-	-	170	28	170	-	73	-	170
EST. FLOW RATE ℓ/sec.	49 | 71 | 89	54	-	-	858	35	858	-	-	-	858
EST. PRESSURE kPa	1275 | 981 | 687	1150	-	-	1380	1212	1380	-	-	-	1380
EST. THROW m	-	90	-	5	170	45	170	-	40	30	170
AT ANGLE DEG.	-	45	-	40	40	-	40	-	-	-	40

CANADIAN MARINE DRILLING LIMITED

SOHIO ICE PAD STUDY

TITLE: SPRAY ICE APPLICATIONS AND APPARATUS

FIGURE No. 6.1

Table 8.2: Summary of Spray Ice Systems (O'Rourke 1984)

APPLICATION		ALERK ISLAND	SOHIO RUBBLE GENERATOR		ESSO BIG GUN EXPERIMENT	SSDC KOGYUK
SPRAY SYSTEM		AURORA	TAIT 100HP	THUNE EUREKA EF400		
NOZZLE FLOW RATE	ℓ/sec.	54	35	858	858	858
NOZZLE PRESSURE	kPa	1150	1212	1380	1380	1380
NOZZLE DIAMETER	mm	38	28	170	170	170
PAD AREA	m^2	5500	20000	20000	NOT FIXED	29000
MEAN TEMPERATURE	°C	-25	–	-28	-21	-38
ELAPSED TIME	SITE DAYS	14	45	4.5	20.3	7.4
PUMP OPERATION	HOURS	240	710	102	305	120
TOTAL WATER SPRAYED	m^3	46474	97000	315000	942000	376000
ESTIMATED ICE PRODUCED	m^3	36000	80000	220000	–	–
% PRODUCED ICE	(VOLUMETRIC)	77	82	70	–	–
ESTIMATED TARGET ICE	m^3	22000	80000	82000	360000	125000
% TARGET RATIO	(VOLUMETRIC)	61	100	37	–	–
% OVERALL EFFICIENCY	(VOLUMETRIC)	47	82	26	38	33
MEASURED SPECIFIC GRAVITY		0.70	0.635	0.614	0.70	0.615
ESTIMATED TARGET ICE	TONNES	15400	50800	50300	252000	76800
% OVERALL EFFICIENCY	(WEIGHT)	33	52	16	27	20
TARGET ICE DEPOSIT RATE:	TONNES/HOUR	64	71	493	826	640
	TONNES/SITE DAY	1100	1130	11200	12400	10400

CANADIAN MARINE DRILLING LIMITED

SOHIO ICE PAD STUDY

TITLE: SPRAY ICE RESULTS

FIGURE No. 6.3

Table 8.3: Summary of Spray Ice System Efficiency (O'Rourke 1984)

A review of field experience of large-scale trials and operational projects has been undertaken to establish operational constraints for spray ice construction. A project undertaken and reported by O'Rourke (1984) made an effort at determining spray efficiency by measuring water and ice volumes for a range of equipment. The basis of this review included:

- Lena River, USSR, 1980: A crossing was constructed across the freshwater Lena River. Spray ice was produced at cold (-32 to –42°C) temperatures using a medium sized pump rated at 75 l/s at 1000kPa pressure. The 1200m long by 40m wide crossing was built in 3 days and deemed suitable for traffic after a further two days of freezing. A thickness of 0.35m was laid on a natural ice base of 0.4m. Three nozzle diameters were used between 35 and 55mm, and it is reported that the smaller nozzle produced a higher ice content, presumable as a function of throw distance and time in the air for heat transfer. Similarly, it is noted that ice content increased linearly with a decrease in temperature and increase in wind speed. It was also noted that unfrozen water would accumulate in low spots and subsequently freeze, adding to the overall ice thickness. Experience gained from 1981 onwards allowed operational procedures to be established to allow jet trajectory, particle size and swing pattern to be varied according to air temperature and wind speed to allow fastest possible ice build-up rates to be maintained.

- Alerk Island, Canadian Beaufort Sea, 1982 (Kemp 1984): An experimental ice pad of 5,500m^3 was constructed on a grounded rubble pile to act as a relief drill pad. A 75 l/sec, 827kPa water cannon was skidded around the periphery of the work site to construct the 83m diameter pad. The experiment lasted 14 days with temperatures ranging between –1 and –40°C, with a mean estimated at –25°C. The jet produced using a 38mm diameter nozzle was capable of projecting the spray 90m at 45° under calm conditions. An ice production efficiency of 47% by volume, 33% by weight was quoted. The spray ice had lower density and salinity that the original ice rubble and seawater, and was considered strong enough to support a drill rig.

- Uviluk, Canadian Beaufort Sea, 1982/83: The SSDC was used as a drilling platform and as a base to support spray ice production equipment for the construction of a relief pad and protection structure at Uviluk. The primary construction method was by flooding, using 6 submersible pumps placed on the ice, rated at 35 l/sec at 240kPa. The construction of berms to prevent loss of unfrozen water allowed all the sprayed volume of water to contribute to the mass of the pad. The low volume capacity of the system was considered insufficient to be used as the sole construction technique, although the ice structure of the berm consisted of natural rubble that formed in late November prior to the start of spraying.

- MV Kigoriak, Mckinley Bay, Canadian Beaufort Sea, 1983/84: This experiment used a large 1000 l/sec fire fighting monitor mounted on the deck of the ice breaker MV Kigoriak. The test site was located within landfast ice, 0.6 to 0.75m thick in 14m water depth with the aim of constructing a stabilized, bottom fast structure. The 20 day trial allowed a total of 305 hours of spray time, resulting in 942,000m^3 throughput. The low spray time was due to high temperatures early in the test, although an average temperature of –21^oC during the last 8 days allowed spraying 24 hours per day. The use of a ship allowed enough flexibility to spray continuously on one of three mounds regardless of wind direction, and the mounds were grounded after about 100 hours of spraying. The use of a spray angle elevation of 60 to 68^o produced optimum results, resulting in an oval of 20m wide by 100 deep while spraying downwind. An overall efficiency of 27% by weight was calculated based on the resulting ice volume.

- Sohio Rubble Generator, McKinley Bay, Canadian Beaufort Sea, 1983/84: This experiment was aimed at generating a rubble pile to act as protection to a drilling structure. A steel structure was grounded in 13m water depth and fitted with two 75kW, 35 l/sec capacity spray monitors. These monitors were used to pump 100,000m^3 of water over 45 days. 51,000 tonnes of ice was produced, suggesting an efficiency of 51% by weight. The MV Kigoriak was then used to complete the ice structure using the "big gun" as described above. This resulted in a doubling of the ice mass in 4.5 days, although at a lower efficiency due to the requirement for accurate placement within the relatively small target. The use of a ship-borne spray system did provide flexibility in placement, particularly in areas which were not well covered by the static pumps due to the predominant wind direction.

- Kogyuk, Canadian Beaufort Sea, 1983/84: The SSDC was used in the same manner as at Uviluk the previous winter, with 12 deck mounted pumps and 6 on-ice submersible units. The small deck mounted pumps produced high porosity ice, which was not able to support the tracked loaders used for leveling, and a method was devised to combine with a flooded technique aimed at producing a stronger saturated ice. The small fire monitor on the Kigoriak was also used for a few days, but was not successful due to high pressure losses in the lines resulting in a weak jet. The use of the "big gun" was more successful and a larger volume of 125,000m^3 of ice was formed in 120 hours of spraying.

Experience from operational ice island construction has built on the early experimental activities, most notably in the 1980s and more recently since 2003.

- Exxon Experimental Ice Island, Prudhoe Bay, 1979/80 (Reimnitz et al, 1982): An ice island was constructed in Stefansson Sound, 6km north of Prudhoe Bay in 3.5m water depth. The island was 400m diameter, and constructed using flooding and spraying techniques. The spray system was used to increase the rate of ice build-up after the surface of the thin landfast ice was initially thickened and strengthened by flooding. The equipment, similar to an irrigation system was rotated about a central pivot and produced a fine mist that partially froze before contact with the island surface. The unfrozen water then ran towards the perimeter of the island, resulting in a dome shaped structure, with 7m freeboard at its centre and 4m at its edge.

- Tarsuit Relief Pad, Canadian Beaufort Sea, 1981/82 (Neth et al 1983): The main source of ice for the relief pad was an ice rubble field that had formed above a previously dredged artificial sand berm. The rubble was moved and leveled using bulldozers, and supplemented by flooded and sprayed ice to achieve the required freeboard. The spray ice was produced by three submersible pumps with a capacity of 21 l/sec, installed at the periphery of the island. These were the same pumps as those used for the Panarctic floating ice islands and at the Uviluk site. An average build-up rate of 70mm/day was achieved to reach the 8m freeboard.

- Cape Alison Spray Ice Pad, Canadian High Arctic, 1984/85 (Masterson et al, 1987): This floating ice platform was constructed on less than 1m thick first year natural sea ice. Four electric submersible pumps were used to build-up the ice thickness to 7m during a construction period of 44 days, a calculated saving of 14 days over flooding techniques. The use of an automatic swivel arrangement contributed to the efficient construction process, by building up 100 to 300mm of ice followed by curing time to allow the ice to reach a temperature of at least $-5^{o}C$ before further spraying at the same location. A total of 6 or 7 spray applications per day were performed in this way to reach the target thickness at an average build-up rate of 136mm/day. Standard flooding techniques were used for the top 0.5m to create a level working surface.

- CIDS Antares Barrier, Harrison Bay, US Beaufort Sea, 1984/85 (Jahns et al, 1986): A horse-shoe shaped grounded ice island protection structure was constructed around the CIDS drilling platform in 14.9m water depth. Three large capacity water monitors of 670 l/sec were mounted on the corners of the platform, which could be controlled in direction and pitch from a central control room. The ice structure was complete in a 60 day construction period, with a total of 4.1 million tonnes of water used to produce 1.6 million tonnes of in-place ice. Construction started when two large multi-year floe fragments became grounded near the platform, which were then surcharged with spray ice and used as

footholds for extending the structure geometry. Thus it was not necessary to wait for full freeze-up before beginning construction activities. Construction was affected by temperature and wind conditions, although the use of three monitors allowed flexibility to optimize spraying as a function of wind direction, and operations were not suspended due to winds. At the end of the drilling program, a path was created through the spray ice structure by jetting with the same high capacity monitors to allow the CIDS to be floated away from the site after break-up. The ice structure was then allowed to deteriorate and finally break-up naturally.

- Mars Prototype Island, Harrison Bay, US Beaufort Sea, 1985 (Sandwell, 2003a): A prototype ice island was constructed in anticipation of exploration, and was used to evaluate construction methods and influence of environmental conditions, as well as provide information on spray ice constitutive behaviour and properties. The island was constructed in 9.1m water depth using two pumps of 240 l/sec and 60 l/sec capacity. The pumps were housed in skid-mounted containers to allow movement around the ice. It was noted that the smaller pump was largely ineffective. Build-up rates of 300 mm/day were measured at the start of construction, increasing to 600 mm/day later as a function of increased experience and equipment modifications. The overall volumetric efficiency achieved during construction was calculated at 43%. The development of a number of cracks was noted during grounding of the island, but only two remained following completion of construction, and they did not remain active.

- Mars Ice Island, Harrison Bay, US Beaufort Sea, 1986/87 (Funegard et al, 1987): The Mars island was the first operational grounded ice island to be constructed using spray ice techniques. Four pumps of 330 l/sec capacity were used during the 45 day construction period. At peak production, 40 pump hours per day was achieved over a 6 day period. A total of 892 pump hours produced 770,000m^3 of ice. The large 37 tonne pump units were difficult to move around on the ice due to freezing in place, partial burial by newly formed ice and difficulty in drilling through the thickening ice.

- Angasak Ice Island, Canadian Beaufort Sea, 1987 (Weaver & Gregor 1988): Four diesel powered skid mounted pumps were used for the construction, with flow rate capacities of 130 and 180 l/sec. A spray and cure approach was taken, with the entire island constructed in uniform lifts of 0.3m to encourage even grounding. The duration of the curing time was established to ensure that the depth of strongly bonded spray ice reached a minimum of 80% of each layer. The warmer than normal ambient temperature during the construction period dictated a change in construction procedure, with thinner layers being applied at each stage, as a function of measured temperature. The use of bulldozers to level the mounds of ice was effective at warmer temperatures, although continuous spraying was considered more efficient below –25^{o}C. A total of 398,000m^3 of water was pumped during the 58 day construction period, producing an average build-up rate of 210mm/day. The development of subvertical tension cracks on

the underside of the spay ice mound prior to grounding, and on the upper surface during and immediately after grounding were observed, but did not adversely affect the performance of the island.

- Nipterk Ice Island, Canadian Beaufort Sea, 1989 (Weaver & Poplin, 1997): Four 200 l/sec pumps were used to produce 860,000m^3 at Nipterk, with a construction duration of 53 days. The island was built in 3 phases; during Phase 1, the rafted first-year ice was covered with 2 to 4m of spray ice to allow sufficient thickness for construction equipment to operate safely. Phase 2 entailed construction and grounding of the core of the island by positioning the pumps about 100m from the island centre and using bulldozers to compact and level the ice. Phase 3 consisted of semi-continuous spraying to complete the working surface and edges of the island. Cracking of the island core was observed during grounding, but the cracks were filled with reworked ice and were not considered to be problematic. A break-down of construction activities showed that the pumps operated for 40% of the time, with down-time associated with mechanical issues (40%), weather (16%) and moving location (3%). A high average efficiency of 105% by volume was noted, with a clear trend of increasing efficiency with reduced temperature. Losses were primarily through evaporation and wind transport, as well as gravity drainage of brine and unfrozen pore water. One of the reasons quoted for a high efficiency was that the location of the island was near the mouth of the Mackenzie Delta, with relatively fresh water.

- Karluk Ice Island, US Beaufort Sea, 1989 (Bugno et al, 1990): Four pump units with a flow rate of 330 l/sec were used to produce 358,000m^3 of spray ice. The original pumps were fitted with vertical turbine pumps and weighed 38 tonnes, which would have required 1m thick floating ice for support. Two of the pumps were modified by replacing the pump with a centrifugal system, which halved the weight and allowed easier maneuvering and positioning on the ice. The island was constructed in 38 days between mid December and mid January using a lift and cure technique. Layers of 0.3 to 0.6m were deposited, followed by a break to allow repositioning of the pumps. The mounds of fresh ice were also spread and leveled during this time. The early construction was undertaken in relatively warm conditions, which limited efficiency, but colder temperature during the second half of the schedule (average –29^{o}C) allowed build-up rates of up to 900mm per day to be achieved. It was noted that nozzle size was an important factor in ice production, and in warm weather, the efficiency of a smaller nozzle more than made up for the lower spray volume. Spraying accounted for only 20% of available time, with the time required for moving the skid pumps and mechanical downtime (11%) quoted as an area for potential improvement through the use of lighter equipment.

- Thetis Ice Islands, Harrison Bay, US Beaufort Sea, 2003 (Sandwell 2003b, Masterson et al 2004): Three spray ice islands were constructed in 2.3 to 3.7m water depth in Harrison Bay using combinations of 190 and 330 l/sec mobile pumps, with two pumps being used on each island. Ice production was

supplemented with ice chips hauled from a nearby onshore production area when weather conditions were not appropriate for spraying. A spray and cure technique was adopted, with curing periods increased in warmer temperature. The construction period for each island ranged from 21 to 42 days, with the first 2 islands being undertaken simultaneously.

- Kashagan Ice Protection Structures, Caspian Sea, 2002/03 (Bastian et al 2004): An ice protection system was deployed to protect offshore installations against ice loading and provide shelter for supply vessels. The system was made up of grounded barges, loaded with spray ice to improve sliding stability. Three pump designs were considered, depending on the weather conditions and location. These systems included a large 330 l/sec fire fighting pump which operated well at temperatures lower than -10^{o}C, a 17 l/sec waterous fire fighting unit for use in temperatures lower than -6^{o}C and an Areco fan system that produced 11 l/sec for use in warm temperatures of 0 to -10^{o}C. The larger pumps produced the required 6000m^3 of spray ice within 40 hours, even though only 6 to 10% of the water sprayed resulted in spray ice on the protection structure.